

AD609717

DYNAMIC ELECTRICAL MODELING OF ELECTRODES MOVING IN SEA WATER

INTERIM REPORT NO. 30-P-7

October 1964

OFFICE OF NAVAL RESEARCH

Washington, D.C.

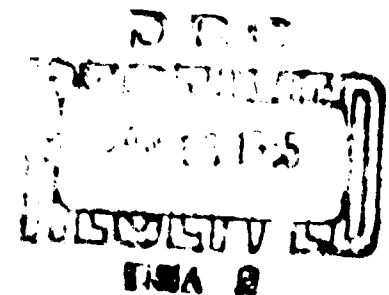
COPY	2	OF	3	TR
HARD COPY	\$. 3.00			
MICROFICHE	\$. 0.75			

61P

CONTRACT NO. NONr 3387(00)

NR 371-590

Dated 15 December 1960



DECO Electronics, Inc.

Boston

Boulder

Leesburg

Washington

ARCHIVE COPY

DYNAMIC ELECTRICAL MODELING OF ELECTRODES
MOVING IN SEA WATER

by
L. Ball

October 1964

REPORT 30-P-7

Office of Naval Research
Washington, D. C.

Contract NOnr 3387(00)

NR 371-590

DECO ELECTRONICS, INC.

Boston Boulder Leesburg Washington, D. C.

TABLE OF CONTENTS

Section	Page
ABSTRACT-----	v
1. INTRODUCTION-----	1
2. BRIEF LITERATURE SURVEY-----	2
2.1 Submerged Antennas-----	2
2.2 Corrosion and Motion Effects-----	3
3. MODELING REQUIREMENTS-----	4
3.1 Noise Level-----	6
3.2 Sensitivity-----	7
3.3 Parametric Control-----	8
4. PROPOSED MODEL SYSTEM-----	9
4.1 General Description-----	9
4.2 Noise Quieting-----	13
4.3 Signal Levels-----	16
4.4 Detection Techniques-----	20
4.5 Dynamical Considerations-----	22
5. SYSTEM CAPABILITIES-----	26
6. ACKNOWLEDGEMENTS-----	28
7. REFERENCES-----	29
APPENDIX A - The Impedance of Cylindrical Electrodes	
in a Conducting Medium-----	A-1
A.1 The Equivalent Spherical Radius	
of a Cylindrical Electrode---	A-1
A.2 The Capacitance and Resistance	
of Two Spheres-----	A-4
A.3 On the Variation of Electrode	
Impedance with Respect to	
Contact Area-----	A-7
Case A Bubble Around the Ends---	A-8
Case B Uniformly Distributed Bubbles	A-10
Interpretation-----	A-11

Section	Page
APPENDIX B - Notes on Cavitation and Electrical Noise-----	B-1
APPENDIX C - Development of an Equivalent Circuit for a Dipole Antenna-----	C-1
APPENDIX D - Voltage Induced into an Electric Dipole Moving in the Earth's Magnetic Field-----	D-1

LIST OF ILLUSTRATIONS

Figure	Illustration	Page
1	Equivalent Circuit of a Dipole Antenna in Sea Water	5
2	Pictorial Diagram of Simulator System	10
3	Cross Sectional Detail of Simulator Test Section	11
4	Signal Detector Block Diagrams	12
5	Typical Colorado Mean Noise Density Spectrum [Maxwell and Stone, 1964] and the Effect of Copper Shielding	14
6	Electromagnetic Properties of Sea Water Having $\sigma = 4$ mhos/meter	17
7	Signal-to-Noise Ratio Improvement by Linear Filtering	23
8	Fluid Velocity Profiles in the Test Section	25
A-1	Equivalent Spherical Radius for a Cylindrical Electrode in a Conducting Medium	A-3
A-2	Capacitance and Conductance Between Two Spheres in a Conducting Medium	A-6
A-3	Impedance of Two Cylindrical Electrodes as a Function of Contact Length/Area; $\sigma = 4$ mhos/meter	A-9
C-1	Equivalent Circuit of a Dipole Antenna in Sea Water	C-4
D-1	Geometry for Wire Oscillating in a Plane Perpendicular to the Earth's Magnetic Field	D-3
D-2	Induced Voltage and Equivalent Electric Field Strength for an Electric Dipole Rotating in the Earth's Magnetic Field	D-5

DYNAMIC ELECTRICAL MODELING OF ELECTRODES

MOVING IN SEA WATER

By

L. Ball

ABSTRACT

This study has direct application to the design of submerged dipole antennas. The hypothetical laboratory modeling system consists of a closed circuit water tunnel capable of simulating the electrodynamic and hydrodynamic properties of water at speeds up to 20 knots. Electrical noise quieting is achieved by shielding and correlation techniques. Only the test section of the water tunnel is shielded. Additional quieting is obtained by using coaxial electrodes. The simulator features parametric control of fluid properties, corrosion rates, turbulence, fluid velocity, model shape and materials.

1. INTRODUCTION

The observation of electromagnetic fields in the oceans using electric dipoles is beset by a number of problems which degrade the dipole performance. This study is concerned with the grounded-end electric dipole antenna which has shown promise as being an extremely useable antenna. Fundamental in the design of this dipole is the attainment of the lowest possible contact impedance at the electrodes and maintaining that impedance under all operating conditions.

An optimum design can be achieved if problems associated with electrical noise and fluid flow can be surmounted. The principle sources of electrical noise are as follows:

- 1) Atmospherics which decrease with depth,
- 2) Thermal noise in the electrode resistance,
- 3) Dynamic water flow noise due to irregularities in the flow past the electrodes,
- 4) External man-made noise such as what might originate at the towing vehicle,
- 5) Noise due to the motion of the dipole in the earth's magnetic field. (See Appendix D)

Since the first and fourth sources are external and not associated explicitly with the design of the electrodes, they may be eliminated as design factors except as they may affect the model study. The second and third sources are not quite independently related, for as it is shown in Appendix A3, the electrode resistance is dependent on the total area in contact with the sea water, and the contact area in a turbulent flow situation is dependent on the relative velocity between the water and the electrode. Thus, the thermal resistance is to a degree dependent on velocity.

To the present time, the principle design procedure has involved trial methods in which various electrode configurations have been

subjected to actual sea tests. This technique suffers the disadvantages of being excessively costly and time consuming, and permits only a low level of control over primary test parameters. Furthermore, the oceans present a very complicated electromagnetic environment where practically all physical parameters are uncontrolled variables. [See Longuet-Higgins, Stern, and Stommel, 1954, and von Arx, 1950].

Thus, there is a recognized need for a method which will permit experimental studies in the laboratory. The method described herein provides a high level of control over critical parameters besides obviating an expensive screen room. This technique permits the experimental dynamic testing of the mechanical and electrical properties of the electrodes under controlled conditions. It is thus possible by varying selected parameters to separate many noise sources which were previously integrated due to a lack of parametric control. This knowledge will be of assistance in the optimum choice of electrode design parameters such as size, shape, and material.

2. BRIEF LITERATURE SURVEY

2.1 Submerged Antennas

There has been a great amount of theoretical and experimental effort in the study of the characteristics of antennas submerged in sea water. Hansen [1963] published an excellent bibliography of pertinent literature in the May 1963 issue of the IEEE Transactions on Antennas and Propagation. This issue has other notable papers which have a bearing on the subject. The grounded-end electric dipole antenna being considered here was apparently first described by Moore [1951] as a coaxial antenna in which the sea water formed the outer conductor. Moore's work was recently augmented by King [1963] in which several antenna configurations including the center-driven insulated antenna with bare ends is considered. The subject of antenna impedance is quantitatively discussed by Gooch, Harrison, King, and Wu [1963].

Experimental studies of submerged antennas have, for the most part, been limited to the static (not moving) type of experiment. Notable in this respect is the work of Iizuka [1963, 1964] , Iizuka and King [1962] , and Blair [1963] . Most of this work is applicable to dipoles having lengths of the order of a quarter wavelength or longer in the conducting medium.

2.2 Corrosion and Motion Effects

Conspicuous by its absence is engineering data on the effect of a moving corrosive medium on the dipole performance. It is well-known that metals immersed in an electrolyte such as sea water develop surface charges during the process of corrosion. If these metals or electrodes are moving in the electrolyte, the variation of surface charge density can be expected to add additional noise. Uhlig [1948, 1963] has pioneered corrosion studies for a number of years. He has demonstrated definite correlations between velocity and corrosion rates as well as publishing definitive works on the effects of dissimilar metals. Other recent publications on corrosion and fouling mechanisms are given by Moeller [1963] , Muraoka [1963] , Hoar [1963] , and Barkan [1960] .

Besides variations in the corrosion rates and potentials, other significant problems demand attention. For example, variations in the ocean's current density, due to waves and currents, is discussed in a paper by Longuet-Higgins, Stern, and Stommel [1954] in which it is shown that these variations affect signals received by towed electrodes in a generally complicated fashion. The method of towing electrodes for the purpose of measuring ocean currents was apparently first analyzed and tried by von Arx [1950] . von Arx experienced considerable difficulty in his electrode design due to electrochemical action and finally had to resort to selection of nearly matched pairs of electrodes based on static electrochemical tests in the laboratory. The electrodes were selected for chemical and physical similarity so that electrochemical potentials on the two electrodes

would cancel. Even the best pairs developed uncanceled potentials so that routine selection and use of electrodes was not possible.

Other motional affects that are important are turbulence, cavitation, and bubbles in general. It is shown in Appendix A that turbulence and cavitation can produce an effective increase in the electrode's impedance, and the fluctuations of the size of these cavities can cause impedance fluctuations, hence, noise sources. Goldhirsh and Moorthy [1964] did a theoretical and laboratory study on the effects of the bubbles and concluded that there may be a very real noise problem in the immediate vicinity of the bubbling that is inconsequential at larger distances.

The net effect of the motion and corrosion problems is a severe degradation on the performance of the theoretical antenna with zero impedance electrodes. It indicates a need for a method by which one can select an optimum electrode configuration to meet any given set of requirements.

3. MODELING REQUIREMENTS

The principle objective is to develop antenna electrodes which, when moved through sea water, will have very low impedance and a low level of noise. It is particularly desirable that the major design and testing be done in the laboratory under controlled conditions to insure the attainment of optimum designs. The design of laboratory experiments is facilitated by a useable equivalent circuit such as is shown in Figure 1. The development of this circuit is given as Appendix C, and the only differences between this circuit and that in Figure C1 is that it has been modified slightly to account for the cylindrical shield which acts as one electrode.

In addition to the equivalent circuit analysis, preliminary knowledge of the principle problems is required. Outstanding in this respect are problems connected with noise, system sensitivity, and parametric control. These

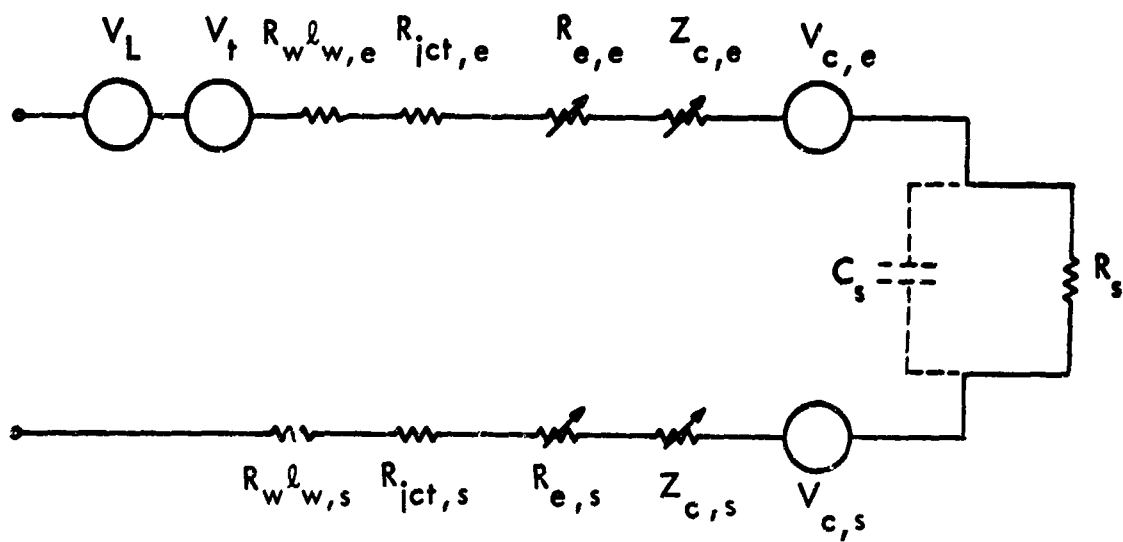


Figure 1 Equivalent Circuit of a Dipole Antenna In Sea Water

In Figure 1,

- V_L = Induced voltage from propagating electric fields
- V_t = Thermal voltage
- $V_{c, e/s}$ = Corrosion potential at electrode/shield
- R_w = Wire resistance per unit length
- $l_{w, e/s}$ = Length of wire going to electrode/shield
- $R_{jct, e/s}$ = Junction resistance at electrode/shield
- $R_{e, e/s}$ = Electrode (metallic) resistance of electrode/shield
- $Z_{c, e/s}$ = Contact impedance of electrode/shield
- R_s, C_s = Resistance and capacitance of fluid between electrode and shield.

problems are also related to the behavior of the equivalent circuit and will be discussed in turn.

3.1 Noise Level

The minimum noise level that will be observed in the system will be the thermal noise generated by the resistive components of the system. If the system is quieted such that thermal noise can be observed, then any level above thermal noise will be observable. Referring to the equivalent circuit, it is expected that the principle resistance will be as a component of Z_c , and this can not be calculated. Based on various corrosion studies, it is felt that a resistance (R_c) of 10 ohms represents a realistic minimum. Wire resistance, $R_w l_w$, junction resistance, R_{jct} , and electrode resistance, R_e , can all be made negligibly small. The resistance due to the lossy medium R_s can be estimated from the transmission line formula [Gray, 1957],

$$R_s = \frac{1}{2\pi\sigma} \ln \frac{b}{a} \text{ ohms/meter}$$

where: σ = fluid conductivity, mhos/meter
 b = Inside radius of shield
 a = Electrode radius.

Using a radius ratio of 20 and a conductivity of 4 mhos/meter, the fluid resistance turns out to be 0.12 ohms/meter, and so this is probably negligible as a thermal generator. The rms thermal noise voltage is given as

$$V_t = [4kTRB]^{1/2}$$

where: k = Boltzmann's constant, 1.38×10^{-23} Joules/ K°
 T = Absolute temperature $\approx 300^\circ K$
 R = Total resistance
 B = Bandwidth of measuring circuit, c/s.

Then, normalizing for a 1 c/s bandwidth, the thermal noise voltage in 10 ohms becomes

$$V_t = 4.06 \times 10^{-10} \text{ volts}/\sqrt{\text{c/s}}$$

The normalized electric field, which if observed across a dipole having an effective length of 1 meter would give the above voltage, is then given as

$$\begin{aligned} E &= 4.06 \times 10^{-10} \text{ volts/meter}/\sqrt{\text{c/s}} \\ &= -194 \text{ db// } 1\text{V/M}/\sqrt{\text{c/s}} \end{aligned}$$

This normalized field level represents the minimum normalized noise level that is expected to be important as a design parameter. Section 4.2 will discuss means by which this relatively quiet level can be obtained in the laboratory.

3.2 Sensitivity

The sensitivity will be taken to mean the smallest signal or noise fluctuation that can be detected at the electrode or electrodes that are under test. In many cases, the signal will be a relative difference resulting from two slightly different test conditions, or in other words, the signal may represent a small difference between two large numbers. For example, the impedance of the electrodes could be measured by observing the potential difference resulting from a current of 1 ampere passing between them. If the velocity were changed by a few knots, there would be a slight impedance change which could be observed if the galvanometer was sensitive enough. Thus, even though the voltages and currents are relatively high, it is the relative differences that determine the system sensitivity.

It is felt that the observation of relative values within $\frac{1}{2}$ db will permit a full and successful test program to be accomplished. This would, for instance, provide a valid comparison of the impedance and noise of a test

electrode compared to some standard such as a blunt shape as a function of velocity.

3.3 Parametric Control

Any useable laboratory instrument must provide for careful control of prescribed parameters. A laboratory modeling system to be used for electrode design should be capable of controlling independent variables such as velocity, model shape and material, and fluid characteristics. The dependent variables such as corrosion, turbulence, impedance, and noise level will result as a function of the independent variables. Listing these separately, we have the following:

Velocity--this is taken to mean the relative velocity between the model (electrode) and the fluid. In the proposed system the fluid will move past a static or dynamic model. For realistic simulation, these velocities should be variable from 0 to about 20 knots (0 to 10 meters/sec).

Model shape and material -- it is recognized that the electrode shape and material have an important bearing on the total performance, and the ability to obtain correlations of shape and material variations with the other variables will perhaps be this system's most valuable asset.

Fluid characteristics -- being able to vary the physical characteristics of the fluid will permit correlations with respect to conductivity, chemical composition, viscosity, and possibly others. It should also be possible to control corrosion by varying the characteristics of the fluid rather than the model material as an added dimension in the material-corrosion problem. It would be possible to control the fluid conductivity (by changing the fluid) over a range of about 2.0 mhos/meter to 4.5 mhos/meter to cover the range of sea water conductivities that may be encountered [Smith-Rose, 1933; Saxton and Lane, 1952; Siedler, 1963; Matthews and Clarke, 1963]. Viscosity is, of course, related to turbulence, cavitation, and the support of free bubbles. Therefore, some of the flow problems can be resolved by correlating with

viscosity. The kinematic viscosity of sea water changes linearly with salinity (hence conductivity), and over the conductivity range suggested above the viscosity will range from about $1.8 \times 10^{+2}$ m²/sec. to 10^{+2} m² /sec. [Gray, 1957]. It is expected that much will be learned about the fluid requirements during the actual testing program, and the above figures are estimates of the magnitudes involved.

4. PROPOSED MODEL SYSTEM

The proposed system is shown as a preliminary sketch in Figure 2. The only design effort to date has been in terms of the major problems involved in demonstrating feasibility, thus detailed design factors such as pipe size and weight have not been considered.

4.1 General Description

The water tunnel is a closed circuit pipe with a pump on one leg. The pump can be an axial motor-pump combination or a centrifugal pump driven by a separate motor. The test section, which is on the opposite leg, is electrically isolated from the rest of the water tunnel except for conduction paths through the water itself. As shown in Figures 2 and 3, this section consists of a coaxial electrode arrangement in which the test electrode is in the center of the pipe. The other electrode is the cylindrical plating jacketing the inside of the test section. The balanced coaxial test section will contribute significantly to the required noise quieting by virtue of being an electrically small antenna for the reception of propagating noise fields. The additional required quieting is obtained with the copper shield which surrounds the test section as shown. "Signals" are detected by means of connections to the center electrode and the shield or coaxial electrode.

Figure 4 shows schemes for using either auto or crosscorrelation to detect the expected low level signals. The autocorrelation scheme is by far the simplest to accomplish but it suffers an attendant lack of sensitivity as

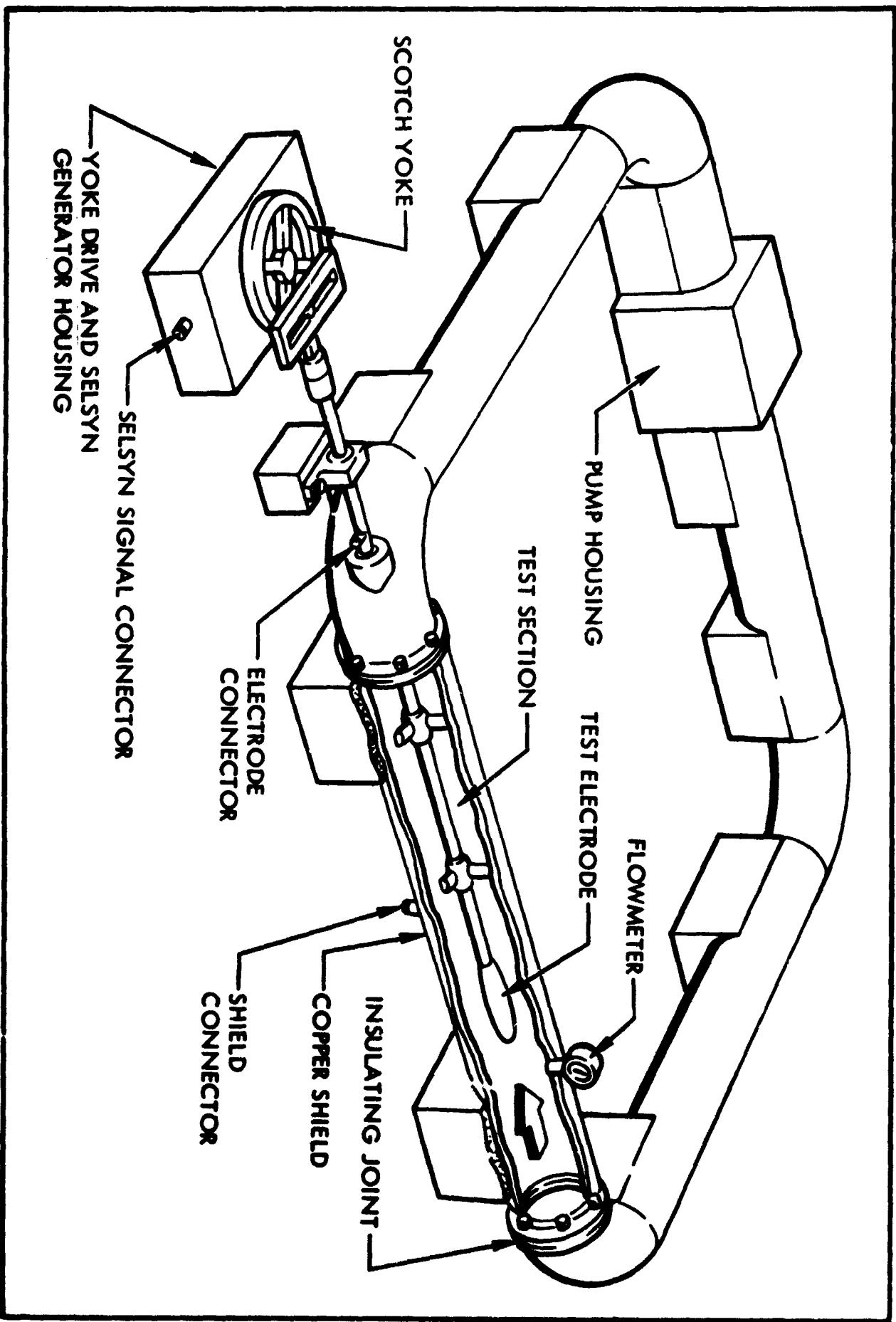


Figure 2 Pictorial Diagram of Simulator System

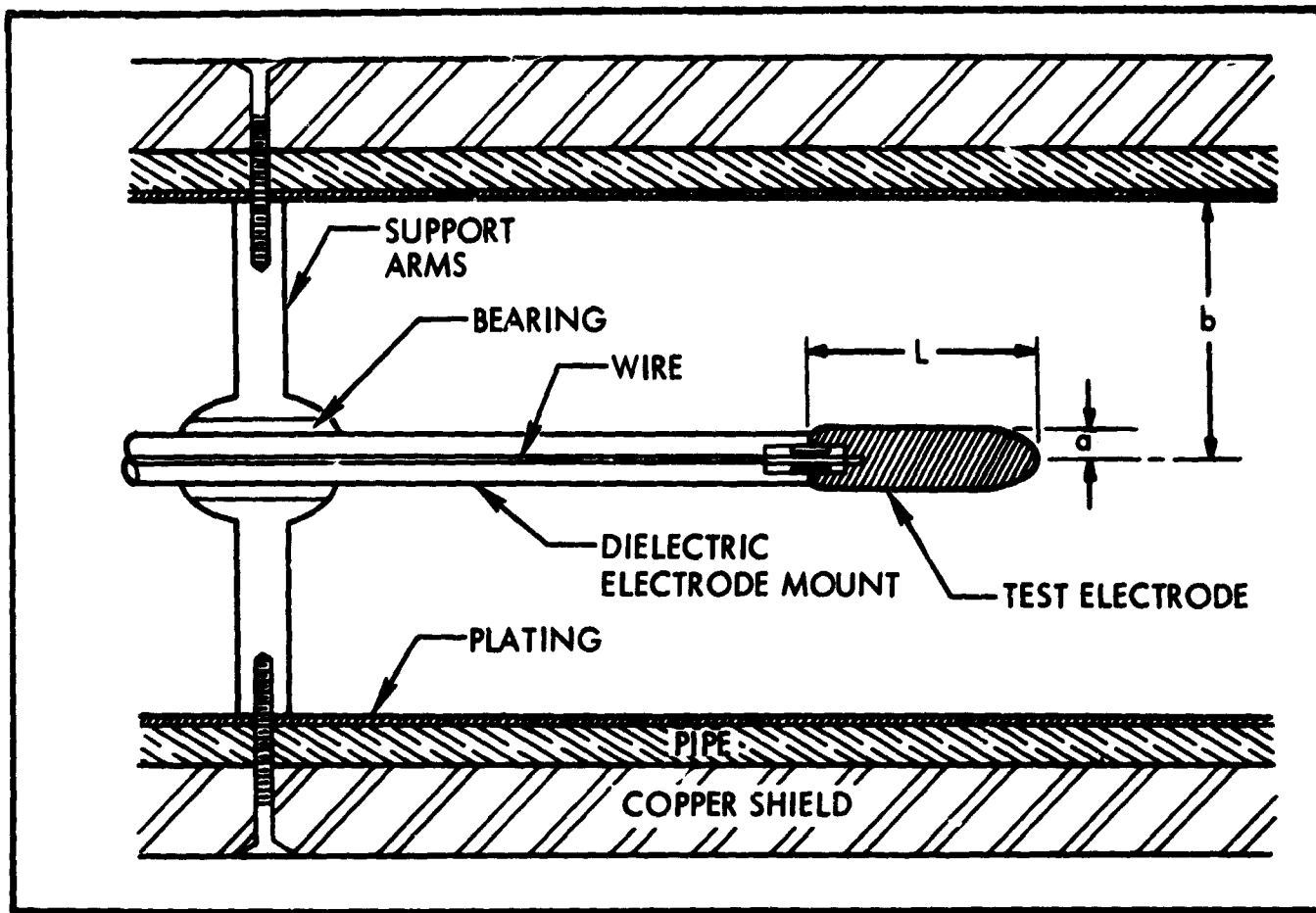


Figure 3 Cross Sectional Detail of Simulator Test Section

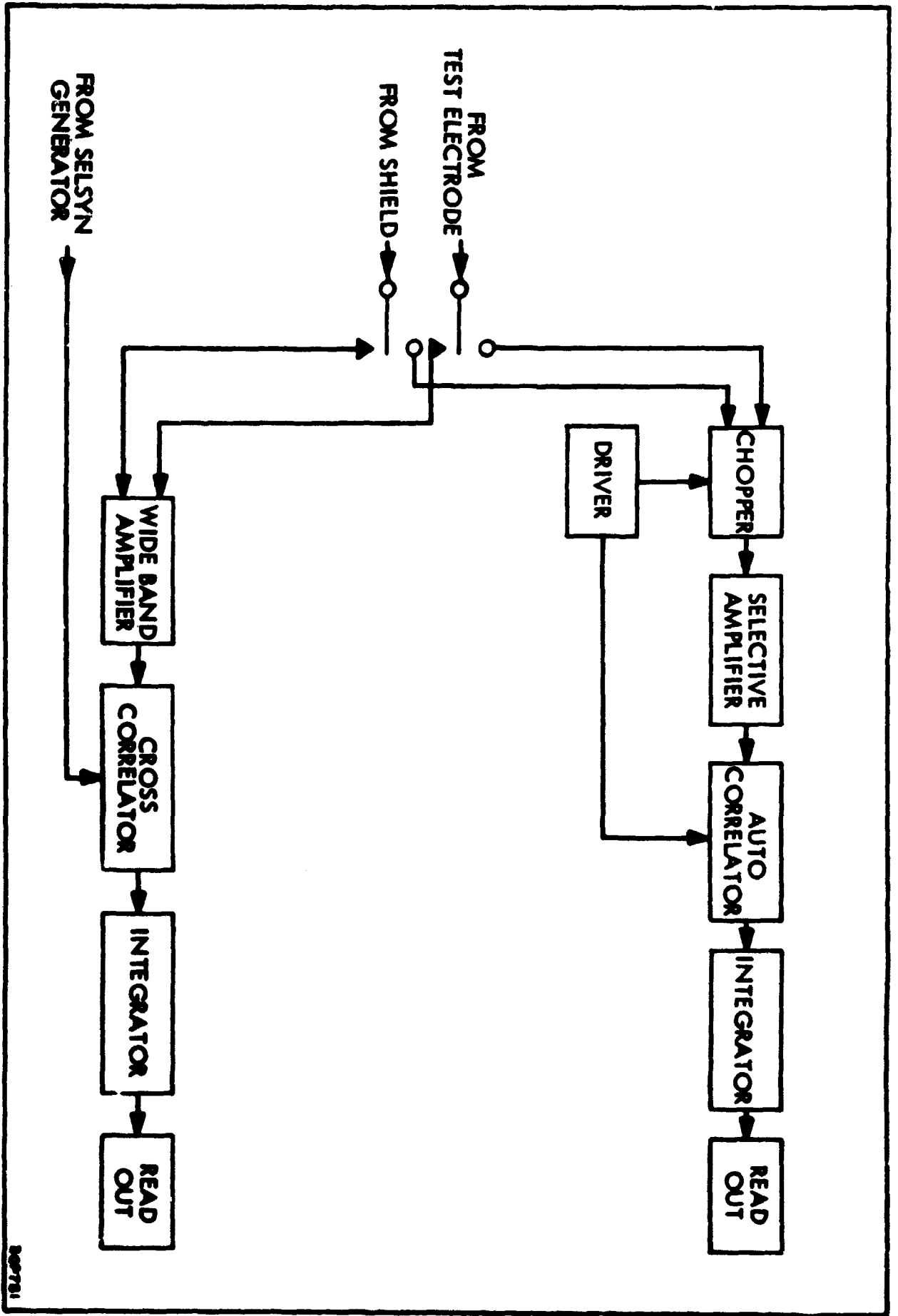


Figure 4 Signal Detector Block Diagrams

100781

compared to the crosscorrelator (this will be discussed in more detail later). The crosscorrelator involves velocity modulation of the center electrode, the angular frequency of which (ω) is detected by a selsyn (or equal) and used as the "local" correlation reference. The velocity modulation is accomplished with a scotch yoke mechanism which imparts an axial simple harmonic motion to the test electrode as shown in Figure 2. Since the impedance between the electrodes is expected to change with the relative velocity, v , there will be an impedance $Z(v, \omega)$. The varying impedance can be observed as a voltage or current variation as a function of v and ω . This varying voltage can then be synchronously detected using the selsyn output as a reference with the result that the read-out will represent the variation of Z with fluid velocity v , or in symbols $Z(v)$.

4.2 Noise Quieting

Perhaps the most formidable problem in the system is the high level of atmospheric and ambient noise which exists near any populated area. The top curve in Figure 5 shows a typical mean noise density spectrum for atmospheric noise which was observed during the summer of 1963 at a rural low-noise site near Boulder, Colorado. Although this site was located about a mile from the nearest commercial power lines, the noise data are typical of that which has been observed at a site only a few hundred yards from the DECO Boulder Laboratory. Hence, the data are representative of noise levels extant at the proposed experimental site. Since the mean noise levels are much higher than the required level, shielding and sophisticated detection techniques must be employed to observe the expected low level signals. The lower curves in Figure 5 show the level of atmospheric noise that would be observed inside of various thickness of copper plate.

Obviously, the expense involved in constructing a sufficiently large shield room with a 300 c/s quieting of 110 db would be prohibitive as evidenced by Figure 5. The present cost of copper is about 50¢ in³ and for the required thicknesses, the costs of the copper shield will range around

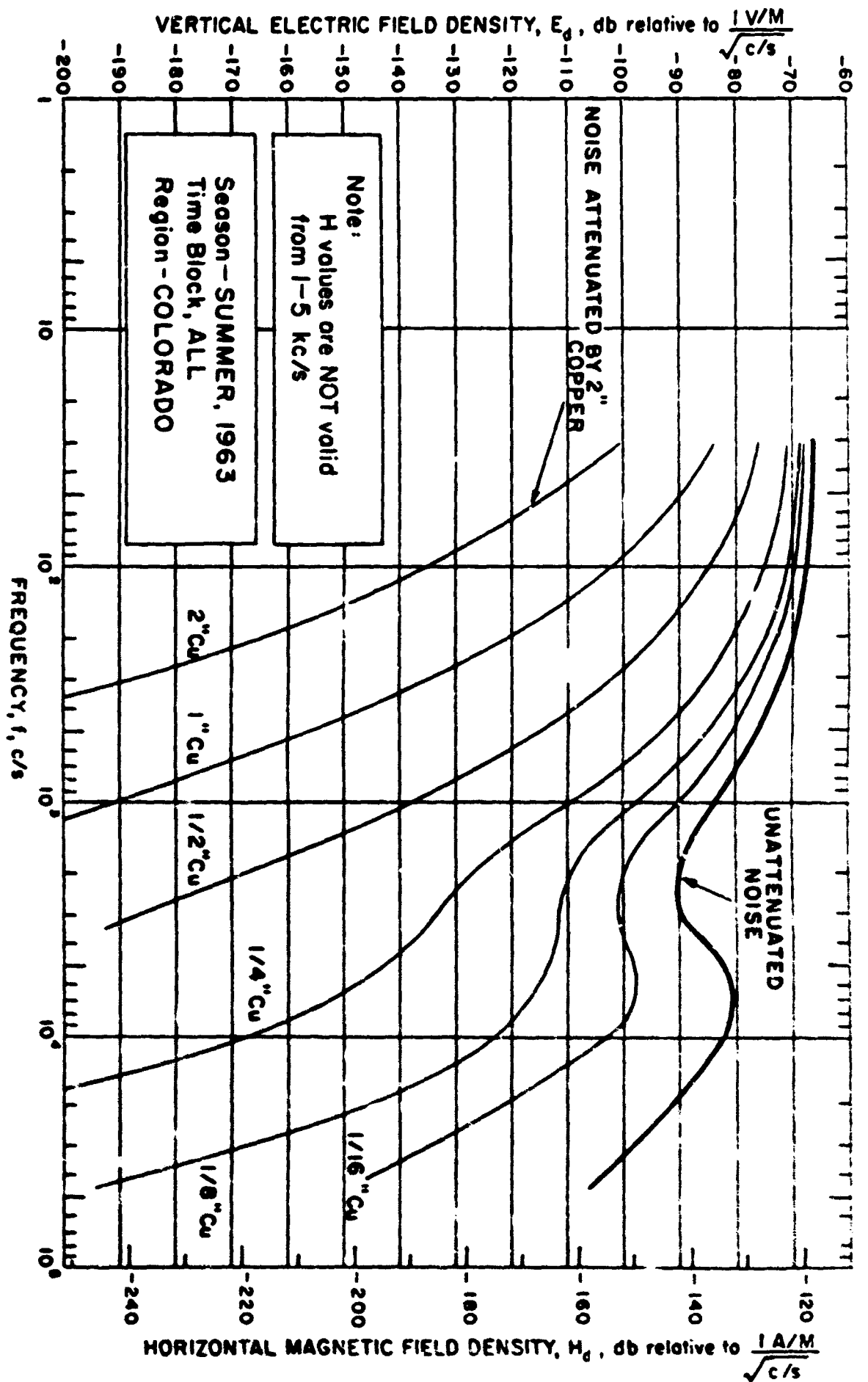


Figure 5 Typical Colorado Mean Noise Density Spectrum [Maxwell and Stone, 1964] and the Effect of Copper Shielding

\$1.00 per square inch of surface area. Now observe in Figure 3 that the test section shown in Figure 2 has a copper shield around the test section itself. There are advantages in this design: 1) the amount of copper required is greatly reduced over that of a screen room, and 2) a highly conducting coaxial electrode is provided. Thus, instead of quieting the whole room, only the important test section is quieted with a significant decrease in cost and increase in available space.

As it was mentioned before, there will be an effective quieting by virtue of the coaxial electrode arrangement. To pick up any noise, the incident field must induce a voltage between the outer and inner electrodes. Since a detailed analysis of the coaxial shielding is quite complicated, it will not be included in this report; however, it can be seen that the induced voltage will necessarily be small by virtue of the low frequency and small spacing (b in Figure 3) between the electrodes. There may be noise pick up on various lead wires that could be troublesome, but by maintaining a balanced system with shielded leads, this can be kept to a minimum.

In addition to the above factors, an effective additional quieting can be obtained through the design of the detectors. This will be discussed in Section 4.4. A quieting on the order of 20 to 40 db can be realized merely by linear filtering, in addition to improvements gained by front-end noise clipping and correlation.

Since the total improvement due to the detection scheme is highly variable, it can not be stated with certainty what levels of quieting are achievable; however, it can be said with reasonable confidence that a normalized noise level of $-180 \text{ db} // 1 \text{ v/m}/\sqrt{\text{c/s}}$ in the test section (including synchronous detection effects) is entirely feasible at frequencies between 100 c/s and 1000 c/s.

4.3 Signal Levels

Referring to Figure 2, the signals that will be observed will be those that exist between the electrode connector and the shield connector. These signals will be either a noise or an impedance variation. When the electrodes are immersed in a corrosive fluid such as salt water, one will also find that corrosion potentials will develop between the two electrodes. It is expected that the impedance as well as these corrosion potentials will vary as a function of the velocity and the characteristics of the moving medium. Excluding the corrosion potentials, it is evident that there will be little or no variation of the impedance as a function of velocity since the impedance of a coaxial-test section is a function of the conductivity, permittivity and the dimensions a and b shown in Figure 3. When the fluid velocity is much less than the phase velocity of an electromagnetic wave in the fluid, there should be no noticeable effect due to the fluid velocity. Referring to Figure 6, note that the phase velocity is greater than 1500 meters per second at any frequency greater than 1 cycle per second. Since the expected test velocities will be on the order of 10 meters per second it is obvious that the fluid velocity should have no significant effect on the impedance, irrespective of corrosion and other external effects. Thus, any impedance variations that do occur are a result of the disturbance of any corrosive films that might have built up on the surfaces of the electrodes. There has been very little published information relative to the electrical effects in a moving fluid, and one of the outstanding features of the system being discussed is that these corrosive effects can be studied analytically in detail, and should lead to a significant contribution to the over-all understanding of the submerged electrodes problem.

The above discussion implicitly assumes that there is a laminar flow existent around the electrodes. However, if this laminar flow is disturbed by turbulence or cavitation, the contact area between the center electrode and the fluid will likely change. Such a change in contact area could

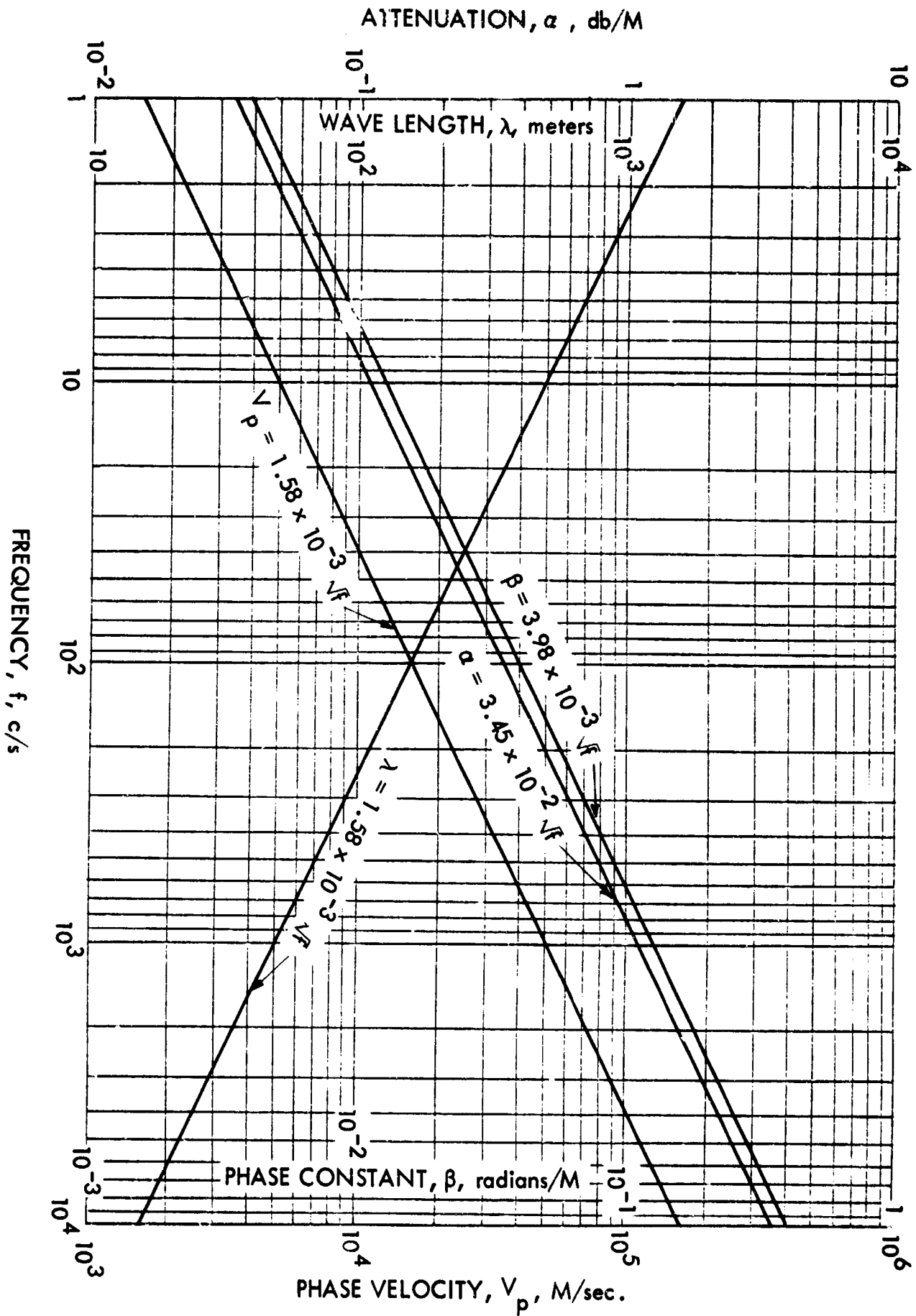


Figure 6 Electromagnetic Properties of Sea Water Having $\sigma = 4$ mhos/meter

result, for instance, from the effect of a blunt electrode sitting in a high velocity fluid. The fluid would set up a turbulence at the leading edge which would bubble round the electrode and could even depart from it, thus, creating a loss of contact area somewhere near the leading edge in the turbulent area. This loss in contact area will lead to a change, in this case an increase in the impedance between the electrode and the conducting medium. Another way in which contact area can be lost is in the case of a rough-surfaced electrode. Surface roughnesses can set up small areas of cavitation which can retain small bubbles on the surface of the electrode. These bubbles will contribute to a total loss of contact area. The effects of these two ways of losing contact area are discussed in detail in the Appendix and it is shown in Figure A3 that there is a significant increase in the impedance ratio as the contact area or length changes. As seen from Figure A3, if the length ratio were to vary from somewhere between 1.0 and 0.8, then the impedance ratio would vary over a range of about 1.5 db. This would also be the same as a variation of any voltages that were existent across two probes. In this case the voltage ratio would be about 1.09 (0.75 db) plus any noise that is existent, thus, the mean level of the voltage fluctuation would be somewhere around 3/4 or a db, which indicates that the system sensitivity should be about 1/2 db.

It is evident from the above discussion that the design of electrodes for laminar flow is extremely important, for if there is as much as 10 percent loss in effective contact length, then, the impedance or given signal levels can vary by as much as a db which represents an extremely troublesome source of noise. This shows that one of the most attractive features of the system is the ability to optimize the hydrodynamic design of any proposed probe configuration.

Since the absolute voltage or impedance levels are expected to be extremely low, this system must be based on the detection of variations in these impedance and voltage levels. It may be inferred from the above

discussions that one of the most important sources of impedance variation lies in the disturbance of the contact impedance between the electrode and the fluid medium. It is seen that this contact impedance depends on the contact area as well as velocity and the chemical constituents of the electrodes and the fluid medium. When any of these factors are disturbed, one can expect to see a change in the impedance of voltage level between the central electrode and the surrounding coaxial shield.

A "worst case" can be discussed by considering terminal voltages due to thermal and atmospheric noise [Maxwell, 1964]. Since the probe system resistance is expected to be on the order of 10 ohms or more, at 300°K in a 10 c/s bandwidth, the rms noise voltage will be

$$v(\text{thermal}) = 1.28 \times 10^{-9} \text{ volts.}$$

From Figure 5, the atmospheric noise field at 300 c/s inside a 2" copper shield is -180 db//1 v/m/ $\sqrt{c/s}$. If this field were observed in a 10 c/s bandwidth with a probe having a voltage effective length of as much as 1 meter, the resulting atmospheric noise voltage would be

$$v(\text{atm}) = 3.16 \times 10^{-9} \text{ volts.}$$

Adding the noise according to the mean square requirement, the total terminal noise voltage is

$$v(\text{noise}) = 3.42 \times 10^{-9} \text{ volts.}$$

Now, suppose that the probe resistance is made to vary by ± 1 ohm by modulating the relative probe/fluid velocity as mentioned earlier. This resistance will cause the thermal noise to take a maximum fluctuation of 0.07×10^{-9} volts. Considering this sinusoidal noise fluctuation to be the signal, the rms signal level is

$$v(\text{signal}) = 0.05 \times 10^{-9} \text{ volts.}$$

This will result in a signal-to-noise (power) ratio of

$$\begin{aligned}\frac{S}{N} &= \frac{[v(\text{signal})]^2}{[v(\text{noise})]^2} \\ &= 2.15 \times 10^{-4} \\ &= -36.7 \text{ db} .\end{aligned}$$

Maxwell has pointed out that the hypothetical case described above is a fair approximation to a worst case S/N for a number of reasons. First, the atmospheric noise level was assumed to have a flat amplitude distribution with frequency when this is known to be untrue. Thus, by making careful measurements of the frequency spectrum of the detected noise envelope as observed at the system output terminals, it should be possible to place the modulating frequency at the point in the spectrum where the noise amplitude is a minimum. DECO presently has the instrumentation for making such a spectrum measurement. Second, the assumption of a 1 meter effective length is probably over estimated by about an order of magnitude, particularly if the probe leads and instrumentation can be shielded for negligible noise pickup. Therefore, it is felt that by careful frequency selection, and instrumentation, that the signal-to-noise ratio can probably be increased by a significant amount. In any case, the level of -36.7 db should be detectable by techniques to be discussed in the next section.

4.4 Detection Techniques

There are several techniques available for detecting signals representative of the performance of the electrodes in the moving fluid. Among these techniques perhaps the simplest is voltage or impedance monitoring with a constant bias current across the probes. These methods are applicable when the input signal-to-noise ratio is equal to or greater than 0 db; however, when the signal-to-noise ratio falls below zero, other techniques such as synchronous detection must be employed. It was shown in Section 4.3 that the signal levels

will, indeed, be quite low, and we shall assume in the discussions to follow that a synchronous detection scheme must be employed.

Two basic types of synchronous detection employ autocorrelation and crosscorrelation. These are shown schematically in Figure 4. Correlation detectors have been discussed in detail by Lee [1960], Lee, Cheatham, and Wiesner [1950], and an electronic correlator has been constructed and tested by Singleton [1950]. The discussion herein will merely summarize the basic, more important, characteristics of these correlators as they are applicable to the system we are considering here.

In the autocorrelation scheme, as shown in Figure 4, the input signals are chopped at some frequency which is used as a reference frequency in the autocorrelation circuit or multiplier. The chopped input is then amplified in a very narrow band amplifier centered on the chopper frequency. This filtered output is then multiplied synchronously with a signal from the chopper driver to give a d. c. output voltage representative of the input signal less noise. The multiplier output is then integrated with a single, long time constant, RC filter and read out on either a voltmeter or some other means. The crosscorrelation circuit, shown in the bottom of Figure 4, requires a separate reference generator, in this case a signal from the selsyn. The output from the crosscorrelator is representative of signals at the input which have the same frequency components as that of the selsyn generator. The integration circuit and readout is the same in both cases. It is seen then that the crosscorrelation circuit requires that the signal be modulated at the same frequency as the reference generator. As shown in Figure 2, this is accomplished by velocity modulating the probe in the moving medium with the scotch yoke setup. The autocorrelation scheme is obviously much simpler to accomplish than the crosscorrelation scheme; however, it has been shown by Lee [1960] that the crosscorrelation, if operated properly, can be significantly more sensitive than the autocorrelator. Hence, if the system is lacking in sensitivity, crosscorrelation may be the

only means by which the characteristics can be measured accurately. Although it is detailed in the literature, suffice it to say here that the crosscorrelation scheme can provide a signal-to-noise improvement of 30 to 40 db over the autocorrelation scheme usually at the cost of time. Such improvements are often quite costly to obtain and require very accurate control over the delay times employed in generating the correlation functions. It is possible that the statistical characteristics of the signal will prohibit significant improvements in the signal-to-noise ratio either by auto or crosscorrelation. Hence, in such cases, the total improvement in the signal-to-noise ratio must be gained by virtue of bandwidth narrowing in the integration circuit. Obviously, the bandwidth of the integrator must be significantly larger than the bandwidth of the signal to prevent signal degradation. Assuming this is the case, Figure 7 shows the improvement that is possible for various integration times. The integration time is taken to be 4 time constants which results in an output representative of the 98.2 percent level of the final ($t = \infty$) value. Thus, for example, if the output signal-to-noise level of 0 db can be read and the input signal-to-noise level is -20 db, then the integration time is slightly over 1 minute. Although an output signal-to-noise level of plus 10 db is very easy to read on most meters, the levels of 0 to -10 db can also be interpreted using "eye-ball integration" techniques and recorders. So, referring again to Figure 7, it can be seen that in integration times of a half hour or less that input signal-to-noise levels of between -20 and -40 db can be detected strictly by integration alone so that any improvements in the correlation scheme itself will add to the over-all system performance. This shows a high confidence level that the low level signals mentioned in Section 4.3 can be detected.

4.5 Dynamical Considerations

Since the purpose of this system is to provide experimental simulation of electrodes moving in sea water, the velocity and flow profiles must be reproduced with reasonable fidelity. This determines the size requirements

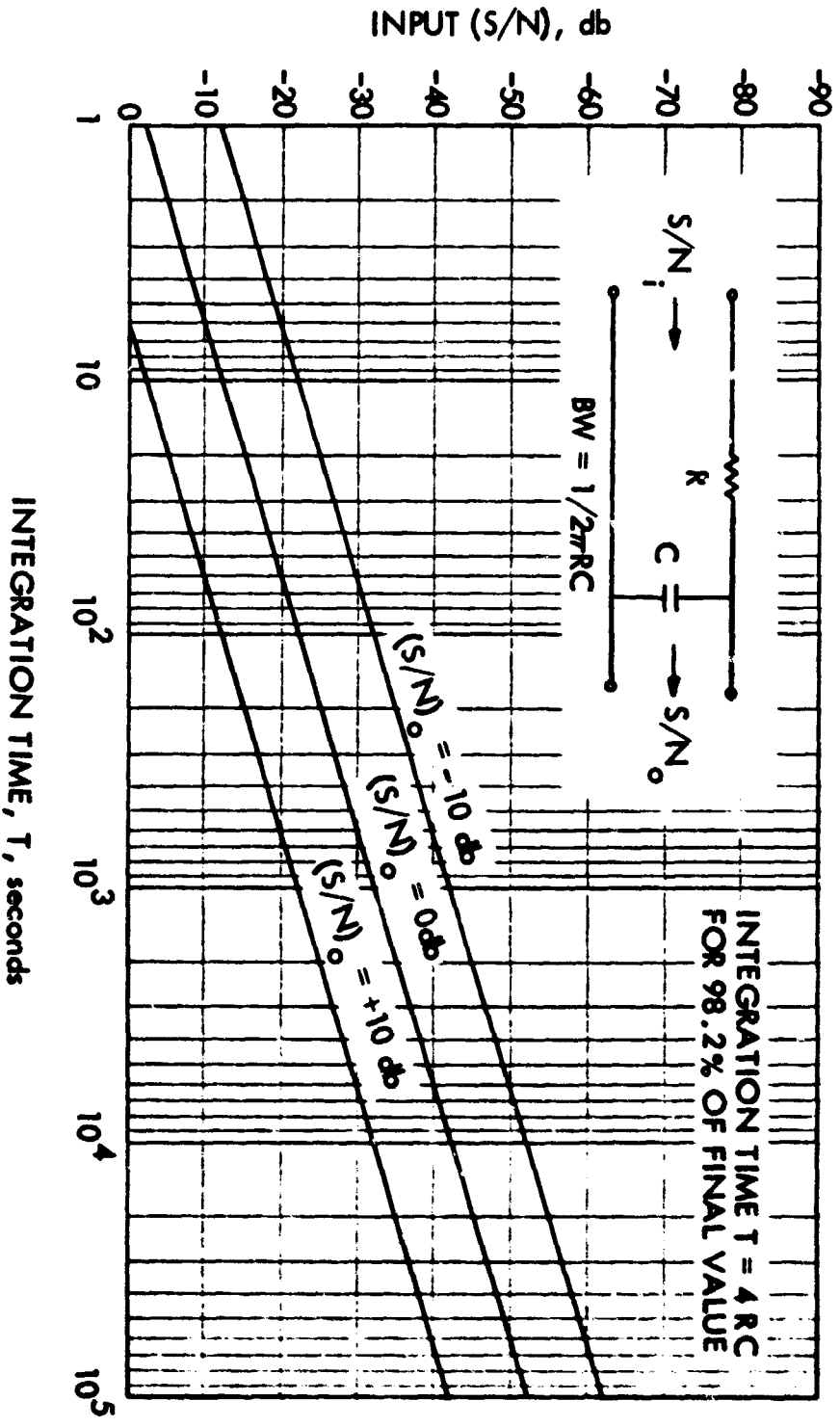


Figure 7 Signal-to-Noise Ratio Improvement by Linear Filtering

for the system as well as most of the flow parameters. One of the important flow parameters is the variation of the pressure along the surface of the electrode. As shown in Appendix B, the localized velocity can become large enough to allow the pressure at the surface to drop below the vapor pressure of the fluid leading to cavitation and turbulence problems. It is shown in Appendix A that such flow problems are a serious degradation to the over-all system performance. The analysis in Appendix D shows the magnitude of potentials that can be induced by erratic movement of the dipole in the earth's magnetic field showing the need for hydrodynamic stability. Obviously, to find the most suitable probe and configurations for any given application, it will be necessary to run exhaustive experiments on probes having configurations varying all the way from extremely blunt to streamlined with possible boundary layer control being incorporated.

An important design factor is the ratio of pipe diameter to electrode diameter. The pipe must be small enough for economy and still large enough to reduce friction and permit high velocity flow, and also large enough to present realistic flow lines in the vicinity of the electrode. Obviously, a rather large diameter ratio is indicated to insure that the velocity profile across the pipe is not significantly disturbed. An estimate of the required diameter ratio can be obtained from the equation of continuity for fluid flow. The quantity of fluid flow Q is the product of area A and velocity. For a full circular pipe,

$$V_o = \frac{Q}{\pi b^2}$$

The velocity V_o can be taken as the mean velocity which for a circular pipe having a parabolic velocity profile is $(1/2) V_{m_o}$ where V_{m_o} is the maximum velocity at the center of the pipe as shown in Figure 8 [Daugherty and Ingersoll, 1954, p. 167]. Since the boundary conditions require that the velocity be zero at the boundary, it is evident that the maximum velocity will increase in the vicinity of the probe assuming, of course, that the flow remains laminar.

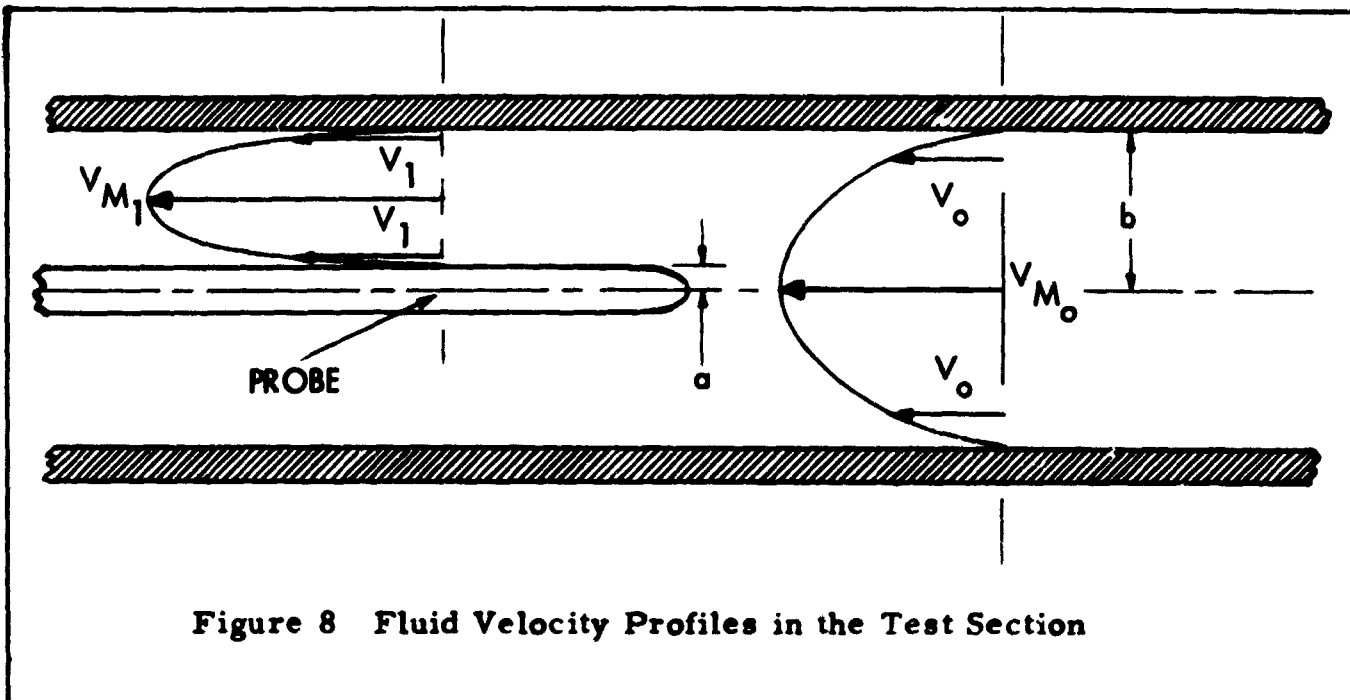


Figure 8 Fluid Velocity Profiles in the Test Section

The desired diameter ratio a/b will be that for which the velocity ratio V_0/V_1 is tolerably close to unity. From the equation of continuity ($Q = AV$) it follows that the velocity ratio can be approximated by

$$\frac{V_0}{V_1} \cong \frac{b^2 - a^2}{b^2} = 1 - \left(\frac{a}{b}\right)^2 .$$

A velocity increase on the order of 10 percent is probably tolerable, and for this range, the equation above gives a diameter ratio b/a of about 3. However, since this calculation was for an ideal laminar flow case, the actual required pipe diameter will be on the order of 15 or 20 electrode diameters to satisfy most of the more complicated flow problems that will arise.

An important dynamic design parameter is the axial stability of the electrode sitting in the high velocity fluid. As shown in Figure 3, the unsupported length of the electrode and mount in front of the first support arms represents a cantilever which could support a self-excited vibration. The amplitude and frequency of such vibrations will be dependent upon the unsupported length, the diameter of the electrode, the mass of the electrode, and the velocity of the fluid. This length-to-diameter ratio will take on a critical maximum for any given electrode mass and fluid velocity. This maximum length-to-diameter ratio will limit the amplitude of the velocity modulation at the scotch yoke mechanism. The critical length-to-diameter ratio is one parameter that will have to be measured experimentally in every given situation. It is evident that such transverse vibrations could ruin an experiment by disturbing the laminar flow boundary along the surface of the electrode, thus, a great deal of care must be exercised in insuring the axial stability of the electrodes in the high velocity medium.

5. SYSTEM CAPABILITIES

In addition to the capabilities mentioned, an obvious and important capability offered by this system is as an aid for the design and construction of electrodes. The achievement of an optimum hydrodynamic and electrodynamic design involves trial design procedures and this system will obviate the necessity for making actual sea tests for performance testing. For example, one could examine the relative performance of various types of materials such as metallic materials with varying degrees of corrosion as compared with nonmetallic conductors such as carbon or other impregnated solids. The hydrodynamic capabilities of this system will also permit evaluation of the composition and construction of any given electrode configuration.

In addition to material selections, it is important to select the configuration to provide electrical as well as hydrodynamic optimization.

Suggested test shapes would include blunt and rough surface shapes varying to shaped and smooth electrodes including a boundary layer control device on the electrode itself.

In addition to the material and shape considerations, this simulator system would also permit the study of the mechanical strength of various configurations. For instance, it may be found that an optimum configuration would tend to vibrate excessively at certain fluid velocities, in which case the fatigue strength of the over-all electrode would become important. Such a parameter could be tested to destruction if necessary with the simulator.

As mentioned in Appendix C, an important antenna parameter is the voltage effective length of the dipole when immersed in its operating medium. It should be possible to measure the effective length of pairs of electrodes set up in the modeling system. For instance, two colinear electrodes can be mounted in the test section and a calibrated electric field could be impressed. The resulting induced voltage measured across the probes would indicate the effective length of the test dipole. Since the dipole separation is expected to be rather large in practice, it probably will be necessary to use a modeled or scaled down dipole for measuring the effective length in the simulator.

The outstanding features of the proposed modeling system become quite apparent when it is realized the extent to which the parameters shown in the equivalent circuit can be separated and studied as separate entities. To summarize, Table 5-1 shows that the parameters shown in the equivalent circuit can be studied by methods which can tend to be independent of one another. The methods suggested in Table 5-1 are merely suggestions as to how the individual parameters can be separated and studied.

TABLE 5-1

<u>Parameter (Fig. C-1)</u>	<u>Method for Studying</u>
1. V_L	Vary shielding parameters; impress a controlled external field
2. V_t	Vary resistance, bandwidth, or temperature
3. V_c	Vary electrode materials; vary fluid properties
4. R_w	Vary length and material
5. R_{jct}	Vary the two materials; vary the sealing at the junction
6. R_e	Vary electrode material and shape
7. Z_e	Related to 3 and 6 above; also vary electrode surface texture
8. R_s, C_s	Vary fluid properties

6. ACKNOWLEDGEMENTS

The author wishes to acknowledge the many productive discussions and helpful suggestions and guidance received from both E. L. Maxwell and A. D. Watt during the process of this investigation. He further thanks the personnel at the USN Underwater Sound Laboratory for their interest and support, in particular that of John Merrill and Marshall Milligan for suggesting the problem and providing valuable background material.

7. REFERENCES

- Barkan, Harold E. (Sept. 1960), "The Nature and Control of Corrosion," Electrical Manufacturing.
- Blair, W. E. (May 1963), "Experimental Verification of Dipole Radiation in a Conducting Half Space," IEEE Trans. on Antennas and Propagation, Vol. AP-11.
- Daugherty, R. L., and A. C. Ingersoll (1954), "Fluid Mechanics with Engineering Applications," (McGraw-Hill Company, Inc.).
- Gooch, D. W., C. W. Harrison, Jr., R. W. P. King, and T. T. Wu (May-June 1963), Impedances of Long Antennas in Air and in Dissipative Media, NBS J. Res., 67D, No. 3.
- Goldhirsh, J., and S. C. Moorthy (June 1963), "Interference Caused by Bubbles Moving in a Current-Carrying Sea-Water Medium," Moore School of Electrical Engineering, Univ. of Pennsylvania, Philadelphia, Penna., Technical Rept. No. 7, Moore School Rept. No. 63-21.
- Gray, Dwight E. (1957), American Institute of Physics Handbook, (McGraw-Hill Company, Inc.)
- Hansen, R. C. (May 1963), "Radiation and Reception with Buried and Submerged Antennas," IEEE Trans. on Antennas and Propagation, AP-11 No. 3.
- Hoar, T. P. (Dec. 1963), "Corrosion," International Science and Technology, No. 24, p. 78.
- Iizuka, K., and R. W. P. King (July 1962), "An Experimental Study of the Half-Wave Dipole Antenna Immersed in a Stratified Conducting Medium," IRE Trans. on Antennas and Propagation, AP-10, No. 4.
- Iizuka, Keigo (Sept. 1963), "An Experimental Study of the Insulated Dipole Antenna Immersed in a Conducting Medium," IEEE Trans. on Antennas and Propagation, AP-11, No. 5, 518.
- Iizuka, Keigo (Jan. 1964), "An Experimental Investigation on the Behavior of the Dipole Antenna near the Interface Between the Conducting Medium and Free Space," IEEE Trans. on Antennas and Propagation, AP-12, No. 1.
- Jordan, E. C. (1961), "Electromagnetic Waves and Radiating Systems," (Prentice Hall, Inc.).

- King, R. W. P. (June 1963), "Theory of the Terminated Insulated Antenna in a Conducting Medium," Tech. Rpt. No. 412, Cruft Laboratory, Harvard University, Cambridge, Mass., Also in IEEE Transactions on Antennas and Propagation, VAP-12, No. 3, (May 1964).
- Lee, Y. W. (1960), "Statistical Theory of Communication," (John Wiley and Sons, Inc., N. Y. and London).
- Lee, Y. W., T. P. Cheatham, Jr., and J. B. Wiesner (Oct. 1950), "Application of Correlation Analysis to the Detection of Periodic Signals in Noise," Proc. of the IRE, 38, No. 10.
- Longuet-Higgins, M. S., M. E. Stern, and Henry Strommel (1954), "The Electrical Field Induced by Ocean Currents and Waves With Applications to the Method of Towed Electrodes," Papers in Physical Oceanography and Meteorology published by Mass. Inst. of Technology and Woods Hole Oceanographic Inst, Vol. III, No. 1, (Nov. 1954).
- Mathews, F. S., and F. C. Clarke (Feb. 1963), "The Electrical, Structural and Topographical Characteristics of Arctic Sea Ice," DECO Electronics, Inc., Rept. No. 52-P-1, 1, Contract NObsr 87687.
- Maxwell, E. L. (1964), Private communication.
- Maxwell, E. L., and D. L. Stone (1964), "ELF and VLF Atmospheric Noise," DECO Rept. No. 30-P-6, DECO Electronics, Inc., Contract No. NONr 3387(00).
- Moeller, Richard (April 1963), "Sea Water Corrosion of Engineering Materials," Undersea Technology.
- Moore, Richard Kerr (June 1951), "The Theory of Radio Communication Between Submerged Submarines," Thesis for Doctor of Phil. Degree at Cornell Univ.
- Muraoka, J. S. (May 1963), "The Effects of Fouling by Deep-Ocean Marine Organisms," Undersea Technology.
- Saxton, J. A., and J. A. Lane (Oct. 1952), "Electrical Properties of Sea Water," Wireless Engineer.
- Siedler, Gerold (1963), "On the In Situ Measurement of Temperature and Electrical Conductivity of Sea-Water," Deep Sea Research, Pergamon Press Ltd., 10, pp. 269-277.

- Singleton, Henry E. (Dec. 1950), "A Digital Electronic Correlator,"
Proc. IRE, 38, No. 12.
- Smith-Rose, R. L. (1933), "The Electrical Properties of Sea Water for
Alternating Currents, Proc. Roy. Soc. A, 143, p. 135.
- Sunde, E. D. (1949), "Earth Conduction Effects in Transmission Systems,"
(D. Van Nostrand Co., Inc.)
- Uhlig, Herbert H. (1948), "The Corrosion Handbook," (John Wiley and Sons,
Inc., New York and Chapman and Hall, Ltd., London).
- Uhlig, Herbert H. (1963), "Corrosion and Corrosion Control, An Introduction
to Corrosion Science and Engineering," (John Wiley and Sons, Inc.,
New York and London).
- vonArx, William S. (March 1950), "An Electromagnetic Method for measuring
the Velocities of Ocean Currents From a Ship Underway," Papers in
Physical Oceanography and Meteorology Published by Mass. Inst. of
Tech. and Woods Hole Oceanographic Inst., Vol. XI, No. 3, (March 1950).

APPENDIX A
THE IMPEDANCE OF CYLINDRICAL ELECTRODES
IN A CONDUCTING MEDIUM

A.1 The Equivalent Spherical Radius of a Cylindrical Electrode

A cylindrical electrode immersed in an infinite conducting medium will see an impedance which is equivalent to that seen by a sphere of radius R_{eq} . An expression for this radius will be derived below.

Since the impedance for a nonferrous medium will be resistive and capacitive, and since the solution for one component will give the other using the duality principles, the expression for R_{eq} will be derived by using the equivalence of capacitances.

The capacitance of an isolated rod was studied by G. W. O. Howe in 1914 and the method (average potential method) has been summarized by Jordan [1961, pp. 56-59]. (Some work on this theory has also been done by Sunde [1949, ch. III].) For a rod of length L , radius a , and carrying a total charge q' , the average potential along the length of the rod is

$$V_{avg} = \frac{q'}{2\pi\epsilon} \left[\frac{a}{L} + \sinh^{-1} \left(\frac{L}{a} \right) - \sqrt{1 + (a/L)^2} \right]. \quad (A-1)$$

The capacitance is then given as

$$C_c = q'L/V_{avg} \text{ farads.}$$

$$C_c = \frac{2\pi \epsilon L}{\frac{a}{L} + \sinh^{-1} \left(\frac{L}{a} \right) - \sqrt{1 + (a/L)^2}} \quad (A-2a)$$

$$C_c = 2\pi \epsilon L/k_c \quad (A-2b)$$

where:

$$k_c = \frac{a}{L} + \sinh^{-1} \left(\frac{L}{a} \right) - \sqrt{1 + (a/L)^2} \quad (\text{A-2c})$$

Since an isolated sphere of radius b has a capacitance of

$$C_s = 4\pi\epsilon b, \quad (\text{A-3})$$

we see immediately by equating Equations (2b) and (3) that

$$R_{eq} = \frac{L}{2k_c} \quad (\text{A-4})$$

$$R'_{eq} = \frac{R_{eq}}{L} = \frac{1}{2k_c} \quad (\text{A-4a})$$

Figure A-1 shows a plot of R'_{eq} as a function of L/a . Note that R_{eq} is independent of the intrinsic properties of the medium.

This concept can easily be extended to the case of two electrodes in either a full or half-space, as follows. It will be shown in Section A. 2 that the resistance seen by an electrode is inverse to the spherical radius, and it can be shown that one electrode in a half-space sees the same resistance as two electrodes in a full-space namely, $1/2\pi\sigma R_{eq}$. (It is properly assumed here that at ELF there is no significant shunting in the air). This may be demonstrated non-rigorously for ideal media by considering that the resistance seen by one electrode in a half-space is $1/2\pi\sigma R_{eq}$ where R_{eq} is an equivalent hemispherical radius. The same electrode in a full space would see half the resistance since the same power is dissipated over twice the area, then $R = 1/4\pi\sigma R_{eq}$ when R_{eq} is the equivalent spherical radius. Extending, two electrodes in a half space see $1/\pi\sigma R_{eq}$, hence two electrodes in a full space see $1/2\pi\sigma R_{eq}$. This is summarized in the following table:

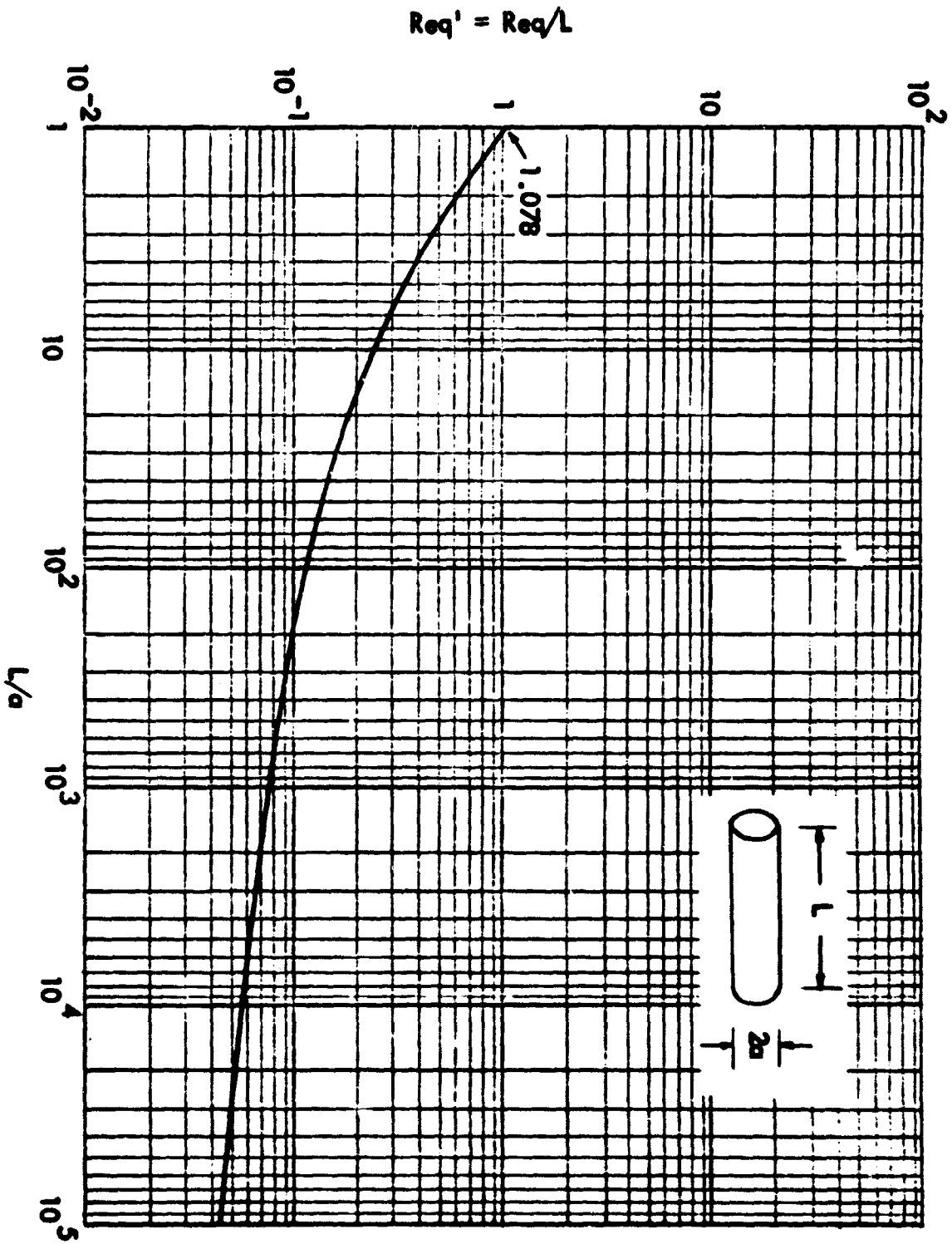


Figure A-1 Equivalent Spherical Radius for a Cylindrical Electrode in a Conducting Medium

RESISTANCE OF ELECTRODES

	<u>Full Space</u>		<u>Half Space</u>	
one electrode:	$\frac{1}{4\pi\sigma R_{eq}}$ (A-5)		$\frac{1}{2\pi\sigma R_{eq}}$	(A-6)
two electrodes:	$\frac{1}{2\pi\sigma R_{eq}}$ (A-7)		$\frac{1}{\pi\sigma R_{eq}}$	(A-8)

It can be seen from the above that R_{eq} is the same for both the full and half-spaces where R_{eq} refers to the radius of the equivalent sphere or hemisphere respectively. In other words, the differences between the impedances in the two spaces is accounted for with the numerical coefficients and not a change in R_{eq} . This means that experimental data for the full space can be approximated with the more easily obtainable half-space data.

As an example, J. J. Jacobson made the following stake impedance measurement in 1961. The stakes were 1/4" Copperweld buried about 1 meter which gives $L/a \approx 314$, and from Figure 1, $R_{eq} \approx 9.1 \times 10^{-2}$ meters. For a ground conductivity of 4×10^{-2} , Equation (8) gives $R \approx 87$ ohms. Jacobson measured a resistance of 69 ohms with an R_{eq} of 6×10^{-2} meters which is comparable with theory. The measurements were undoubtedly affected by stake contact impedance problems. Obviously, much more substantiating data is required.

A. 2 The Capacitance and Resistance of Two Spheres

The impedance seen by two electrodes in a conducting medium can be approximated by the two sphere problem by considering each electrode to have an equivalent spherical surface in an electrical sense. The impedance between the electrodes will be represented as a capacitance in parallel with a resistance.

Consider two spheres having radius b and center-to-center spacing d . The capacitance is given as [Gray, 1957, pp 5-12 to 5-14]

$$C = 2\pi \epsilon b \sinh \beta \sum_{n=1}^{\infty} [\operatorname{csch} (2n - 1) \beta + \operatorname{csch} 2n\beta] \quad (\text{A-9})$$

where $\cosh \beta = d/2b$.

The limiting value of Equation (A-9) is given as

$$C = 2\pi \epsilon b, \quad d \rightarrow \infty. \quad (\text{A-10})$$

Equation (A-9) is plotted in normalized coordinates in Figure A-2.

Here it can be seen that the capacitance is within 10 percent of the terminal value at a spacing of 5 diameters.

The resistance can be obtained by using the principle of duality as follows:

$$\text{If} \quad C = \frac{\epsilon \pi}{k}, \quad (\text{A-11})$$

$$\text{then} \quad R_s = \frac{k}{\sigma \pi}. \quad (\text{A-12})$$

From Equation (A-9) we see that

$$1/k = 2bf(\beta);$$

where

$$f(\beta) = \sinh \beta \sum_{n=1}^{\infty} [\operatorname{csch} (2n - 1) \beta + \operatorname{csch} 2n\beta] \quad (\text{A-13})$$

thus,

$$R_s = \frac{1}{2\pi b \sigma f(\beta)}. \quad (\text{A-14})$$

It can be shown that

$$\lim_{d/2b \rightarrow \infty} f(\beta) = 1 \quad (\text{A-15})$$

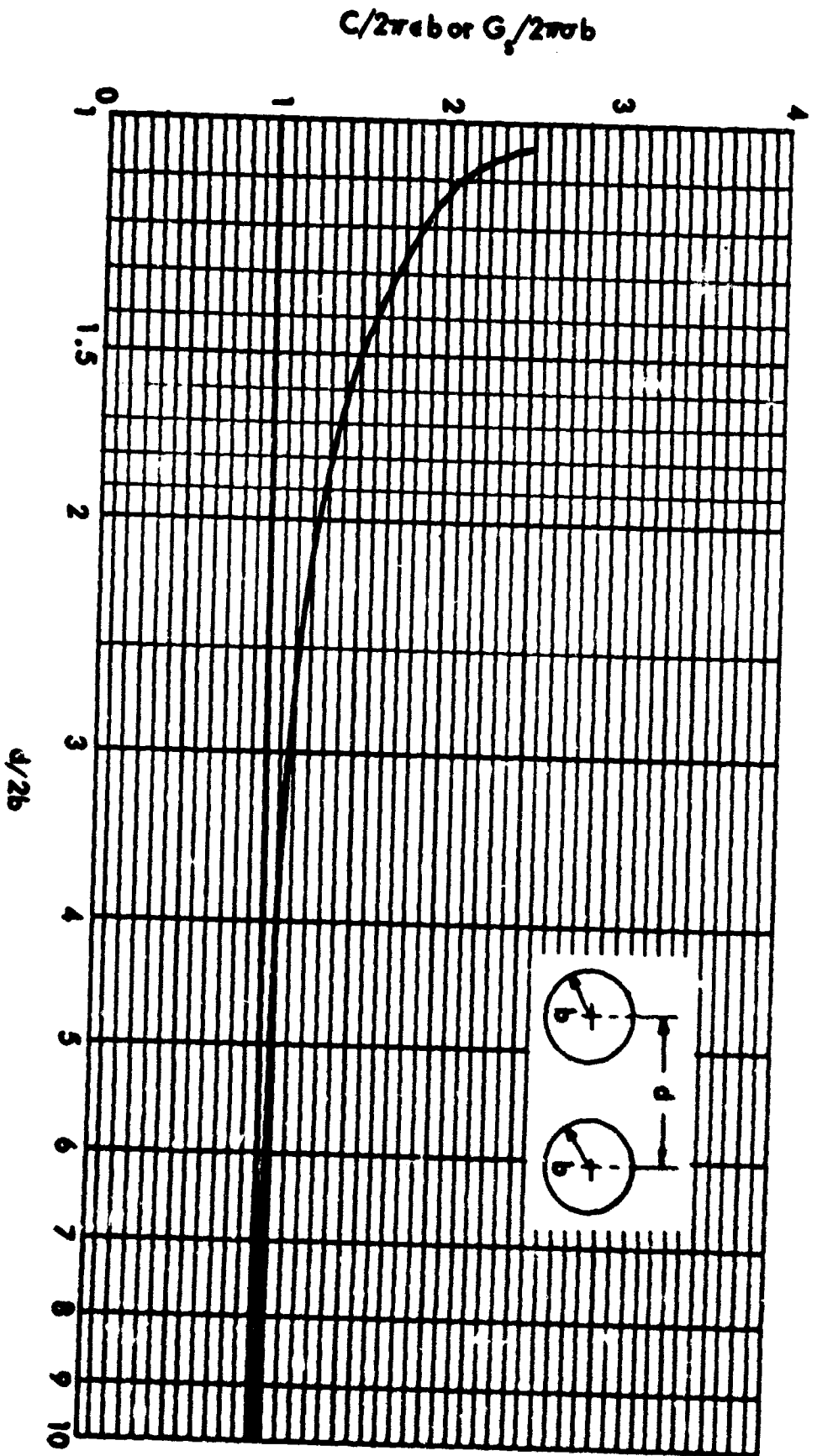


Figure A-2 Capacitance and Conductance Between Two Spheres in a Conducting Medium

and thus,

$$R_s = \frac{1}{2\pi b \sigma}, \quad d \rightarrow \infty. \quad (\text{A-16})$$

Therefore the behavior of R_s is entirely analogous to the behavior of the capacitance. Note that

$$\begin{aligned} C / 2\pi \epsilon b &= f(\beta) \\ G_s / 2\pi \sigma b &= f(\beta). \end{aligned}$$

It is instructive to examine the admittance seen by the two spheres. This is given as

$$\begin{aligned} Y_s &= G_s + j\omega C \\ &= 2\pi b f(\beta) (\sigma + j\omega \epsilon) \\ &= 2\pi b \sigma f(\beta), \quad \sigma \gg \omega \epsilon. \end{aligned}$$

Thus it is seen that there is no significant reactive component in the impedance of the sea for the case considered. If reactive components are observed, they will be attributed to the electrodes and the nature of the corrosive contacts. Furthermore, for typical sea water having $\sigma = 4$ mho/meter,

$$Y_s \approx 25 R_{eq}$$

or

$$Z_s \approx 0.04 / R_{eq}, \quad d / 2R_{eq} > 5 \quad (\text{A-17})$$

where R is the equivalent spherical radius for the electrodes as given by Equation (A-4).

A. 3 On the Variation of Electrode Impedance with Respect to Contact Area

A cylindrical electrode moving longitudinally (in its axial direction) through sea water is likely to experience a variation in the contact area due

to turbulence and cavitation. The resulting impedance variation can be approximated by using the equivalent sphere approach described previously.

Two cases will be described; first, the case (case A) of a blunt ended cylinder in which a cavitation bubble forms uniformly around the end of the electrodes such that the electrode's contact length is shortened. Then, we shall compare (case B) an electrode having a rough surface such that small cavitation bubbles are distributed quasi-uniformly over the entire surface resulting in a decrease in contact area.

The results for the two cases is shown in Figure A-3, in which the sub "o" refers to the original or unchanged parameter. In both cases, the content of the bubbles is assumed to be air.

Case A--Bubble Around the Ends

It was shown in Sections A1 and A2 that the impedance of the two electrodes in sea water having $\sigma = 4$ mho/meter is

$$Z = (4 \times 10^{-2}) / R_{eq} \quad (A-18)$$

where

$$R_{eq} = L / 2k_c$$

$$k_c = \frac{a}{L} + \sinh^{-1} \left(\frac{L}{a} \right) - \sqrt{1 + (a/L)^2}$$

Let

$$R'_{eq} = R_{eq} / L \text{ (Figure A-1)}$$

Then

$$Z = (4 \times 10^{-2}) / R'_{eq} L. \quad (A-19)$$

If the bubble encircling the end of the electrode reduces the contact length by $p = L/L_o$, then the change in impedance is given as

$$Z/Z_o = R'_{eq_o} / (R'_{eq} p). \quad (A-20)$$

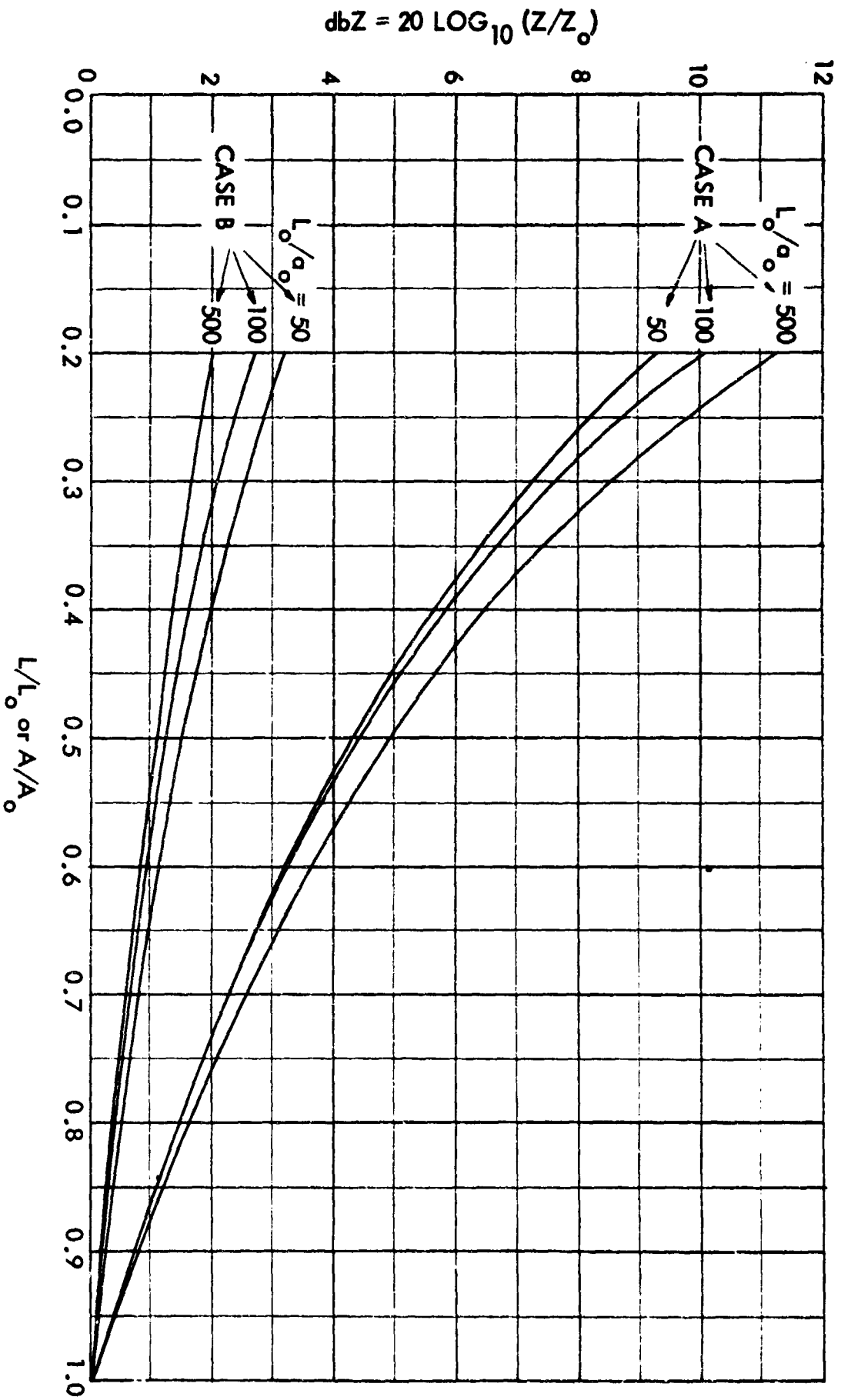


Figure A-3 Impedance of Two Cylindrical Electrodes as a Function of Contact Length/Area; $\sigma = 4$ mhos/meter.

The calculation of Equation (A-20) is shown in Figure A-3 as the Case A curves. Note that each curve is for a constant L_o/a and that the radius a remains constant as L changes. In other words, all the data is normalized with respect to the original unchanged parameters. The physical realization of the curves for $L/L_o < 0.5$ is doubtful and they are shown only for completeness.

Case B--Uniformly Distributed Bubbles

When $L \gg a$, the area of the ends of the cylinder can be neglected compared to the area of the cylindrical surface, and the bubbles will be assumed to be attached to a smooth surface having an area $A_o = 2\pi a_o L_o$. The effect of the decrease in contact area due to the quasi-uniform bubble distribution can be treated as decrease in the cylindrical radius a such that the smaller cylinder will have the same contact area without bubbles as the original cylinder had with bubbles. Let the new contact area b given as

$$A = qA_o \quad (A-21)$$

Then

$$a = qa_o$$

The equivalent spherical radii are now given as

$$\begin{aligned} R'_{eq_o} &= \frac{1}{2k_{c_o}} \\ R'_{eq} &= \frac{1}{2k_c} \end{aligned} \quad (A-22)$$

where

$$\begin{aligned} k_{c_o} &= \frac{a_o}{L_o} + \sinh^{-1} \left(\frac{L_o}{a_o} \right) - \sqrt{1 + (a_o/L_o)^2} \\ k_c &= \frac{a}{L_o} + \sinh^{-1} \left(\frac{L_o}{a} \right) - \sqrt{1 + (a/L_o)^2} \end{aligned} \quad (A-23)$$

The impedance ratio for Case B is seen to be

$$Z/Z_o = R'_{eq_o} / R'_{eq} \quad (A-24)$$

The calculation of Equation (A-24) is shown in Figure A-3 as the Case B curves. Note that there is no ambiguity involved in using either the length or area ratios for the abscissa.

Interpretation

Figure A-3 shows that for blunt electrodes, the impedance will be increased by about 3 db when the contact length or area is reduced by 60-65 percent (Case A). On the other hand, if there were no blunt nose effects, but the same contact area was lost uniformly over the electrode due to surface roughness, the impedance would be changed by only about 1 db. Further, it is seen from the slopes that the impedance is much more sensitive to the blunt nose type of turbulence than to the distributed type.

Generally, there is a definite advantage to designing the electrodes such that there will be no loss of contact area due to turbulence or cavitation. Not only will the impedance be increased, but in a dynamic situation, the size of the bubbles will often fluctuate causing an impedance fluctuation which will lead to a significantly higher noise level. Therefore, if some drag must be introduced, it is much more desirable from the standpoint of noise to distribute the drag uniformly over the electrode surface rather than to use blunt leading edges. Thus one may well expect that no matter where the electrodes are located or what they are made of, they will operate more quietly if the fluid flow is kept as nearly laminar as possible.

APPENDIX B

NOTES ON CAVITATION AND ELECTRICAL NOISE

The purpose of this Appendix is to investigate some of the physical, chemical, and electrical properties of a cavitated fluid such as sea water.

Bernoulli's theorem for a frictionless incompressible fluid, states that the total energy level in a moving fluid is a constant. In other words, the sum of the pressure, static, and velocity heads is a constant. Thus,

$$\frac{p}{w} + Z + \frac{V^2}{2g} = \text{constant} \quad (\text{B1})$$

where:

p = pressure, lbs/square foot

w = specific weight of fluid flowing, lbs/cubic foot

Z = elevation above datum

V = fluid velocity, feet/second

g = acceleration of gravity, feet/second².

According to Equation (B1), if Z is constant and the velocity is increased, the pressure at a point must decrease. The minimum absolute pressure for a liquid is the vapor pressure, p_v , which depends on the liquid and the temperature. If the pressure at a point in a liquid is reduced to p_v or less, the liquid vaporizes (boils) at that point with the resultant formation of vapor bubbles. This is called cavitation. When these bubbles collapse after a sufficient increase in pressure, a very high dynamic pressure is developed at the point (on the order of thousands of atmospheres [Gray, 1957 p2-182 to 2-189]). This high pressure is very destructive to nearby materials and often results in severe pitting. Cavitation is manifested in both minute transient cavities and larger steady state cavities.

A coefficient which is useful for expressing the tendency for a liquid to cavitate is called the coefficient of cavitation which is given as [Daugherty and Ingersoll, 1954, p94, p407] .

$$K = \frac{p_o - p_v}{\rho v_o^2 / 2} \quad (B2)$$

where:

p_o = pressure in the undisturbed flow,

p_v = vapor pressure

ρ = liquid density per unit volume

v_o = relative velocity of liquid with respect to the surface where cavitation is starting.

At some point on the disturbing surface (e. g. a vane), the pressure must have a minimum value and this is usually at a point where the velocity is high and the flow tends to depart from the surface. Letting p_m denote this minimum pressure we have

$$K_i = \frac{p_o - p_m}{\rho v_o^2 / 2} \quad (B3)$$

K_i is a function of the vane design and is usually determined experimentally. If $K > K_i$, then $p_m > p_v$ and cavitation will not ensue. But if $K = K_i$ then cavitation is incipient. The lower the value of K_i , the better the vane is from the cavitation standpoint. If p_o or v_o are such as to make $K < K_i$, the cavitation will be more severe and will increase as K continues to decrease. Other energy relations can be given which are useful for cavitation studies [Daugherty and Ingersoll, 1954].

Cavitation generally originates with the growth of undissolved vapor or gas nuclei existing in the liquid or trapped on microscopic foreign particles [Gray, 1957]. As a result, the growth of the cavity is dependent not only on K but also on viscosity, surface tension, and the presence of surface active materials (detergents, etc.).

Transient bubble cavities [Gray, 1957] are individual bubbles which grow, sometimes oscillate, then collapse, these transient cavities produce very high pressures with periods of the order of a microsecond. These, thus,

contribute to acoustic noise. Any electrical noise which would result would arise from chemical reactions which may be precipitated by the pressure changes.

Steady-state cavities [Gray, 1957] are large stationary cavities which are observed behind blunt obstacles and on hydrofoil profiles with relatively sharp leading edges. While such cavities are, especially at low values of K , usually filled with vapor phase and other gas, they are often observed to contain a mixture of individual bubbles and liquid phase.

Electrical noise resulting from cavitation is likely to arise from molecular and ionic dissociation and recombination as the fluid passes from liquid to vapor phase and back again at the cavity walls. This may or may not be significant since a salted solution is ionized and there may not be any ionic activity associated with a change of phase. Some of the vapors are known to change to a gaseous state which change would be associated with the liberation of high mobility ions. Thus, the change to the gaseous state is likely to be a source of electrical noise. More research into this particular area will be required before the character of the noise can be estimated.

APPENDIX C
DEVELOPMENT OF AN EQUIVALENT CIRCUIT
FOR A DIPOLE ANTENNA IN SEA WATER

In engineering studies of antenna phenomena, it is often convenient to derive a theoretical circuit which under certain prescribed limitations, displays properties equivalent to those of the actual antenna immersed in its operating medium. Such an equivalent circuit facilitates analysis by separating properties such as voltage sources and impedance components into lumped elements which can be studied separately.

The dipole being considered here is shown in Figure C-1 along with a simplified equivalent circuit. The cylindrical electrodes are colinear and separated a nominal distance l . The electrodes are connected to the antenna terminals with insulated wire. The junction between the wire and the electrode may not be sufficiently well protected from the sea water so that dissimilar metal potentials may be a problem. A typical sea-water medium will be assumed to be moving parallel to the electrodes with a relative velocity, V . In some cases a static model will be more satisfactory, but in general the dynamic (relative motion) model will be assumed. In addition, the existence of some natural and man-made fields in the vicinity of the antenna will be assumed, and operating frequencies will be chosen to be 500 cycles per second or less.

A passive no-source circuit will be considered first. Starting at the antenna terminals the first component seen is the lead wires with length, l_w , and total impedance, $Z_w l_w$. This impedance is characterized principally by the per-unit-length wire resistance, R_w , since at these frequencies the inductance and capacitance are negligible. At the point that the twisted wires join an electrode, there is a junction impedance, R_{jct} , which will be assumed to be resistive. It has been shown experimentally that this junction must be hermetically sealed from the sea water to avoid generating

extremely high potentials at the dissimilar metal junction. In general, if the junction is well sealed this particular resistance will probably be negligibly small.

The electrode itself will have an internal impedance due to its material and its form factor. When the electrode is immersed in a corrosive medium, its size will probably be changing and, hence, the impedance is shown as a variable, R_e . In passing from the electrode to the sea water, the current crosses a corroding boundary, the physical chemistry of which is not at all well understood. The contact impedance will be time varying due to chemical corrosion, and will be associated with the all important corrosion potential, V_c , which will be mentioned later. The impedance is expected to be mostly resistive; however, a significant reactive component may be encountered particularly when charged films build up in the process of corrosion. Of particular importance is the variation of the contact impedance due to fluid motion and bubbles in the contact area between the electrode and the water. The contact impedance is probably the largest contributor to the over-all sensor impedance.

The next element seen is the impedance of the sea water in the region of the electrodes. This problem has been analyzed in some detail in Appendix A of this report. It is seen from the formulas derived there that the shunt capacitive reactance is negligible for frequencies of 1000 cycles and less, and the shunt resistance, R_g , is very small on the order of 10 ohms or less in the same frequency band. In other words, the low resistance acts as an effective short circuit for the relatively high capacitive reactance. These approximations apply when the spacing between the electrodes is several equivalent-spherical radii or more as shown in Appendix A.

The return circuit will be almost the same except for a few exceptions. First, the contact impedance may be different by virtue of the difference between anodic and cathodic reactions. Second, the electrode resistance may

be different because of both anodic/cathodic differences and differences in the corrosion rates due to differences in the electrode materials. Third, the return current will see a wire resistance, $R_w l$, do the length of wire between the electrodes as shown in Figure C-1.

Terminal voltages will arise for a number of reasons in each of the major sections of the antenna. The sources can be classified as follows:

- a. Sources internal to the antenna;
- b. Emf's generated at the antenna-medium boundary;
- c. Natural and man-made fields external to the antenna.

The sources internal to the antenna structure will primarily be the thermal noise generated in resistive elements. In Figure C-1, the total effect of all thermal noise generators has been shown as the single voltage generator, V_t . Since the mean-square-thermal voltage is directly proportional to the resistance, temperature, and bandwidth, these voltage sources can be studied effectively by virtue of resistance, temperature, and bandwidth variations.

Emf's which are generated at the antenna-medium boundary, are principally electrolytic in nature. These are shown as V_c in Figure C-1. These electrolytic films represent a serious performance degradation factor since they tend to vary with time as well as with fluid velocity resulting in a terminal voltage high enough to mask any desirable low-level signal. The exact nature of these corrosion potentials has till now been quite indefinite; however, the apparatus described in this report will make the study of these illusive potentials a very ordered and systemic process with the result that electrodes can now be optimized for both material and configuration.

The last principal potential source is that due to natural and man-made fields external to the antenna. The resulting voltage across the antenna terminals will be directly proportional to the magnitude of the field and the effective height of the sensing element. In this case, the sensing elements

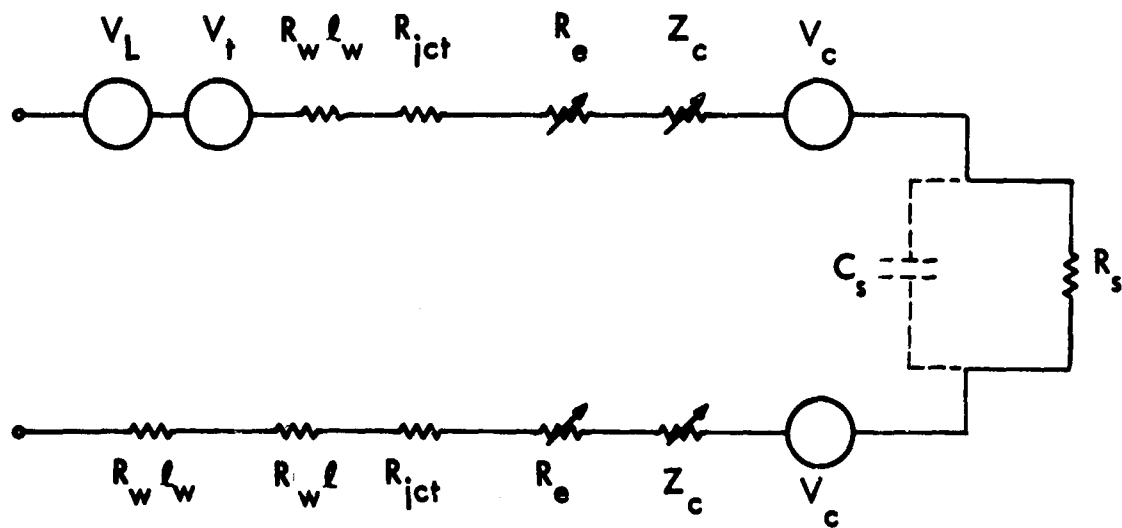
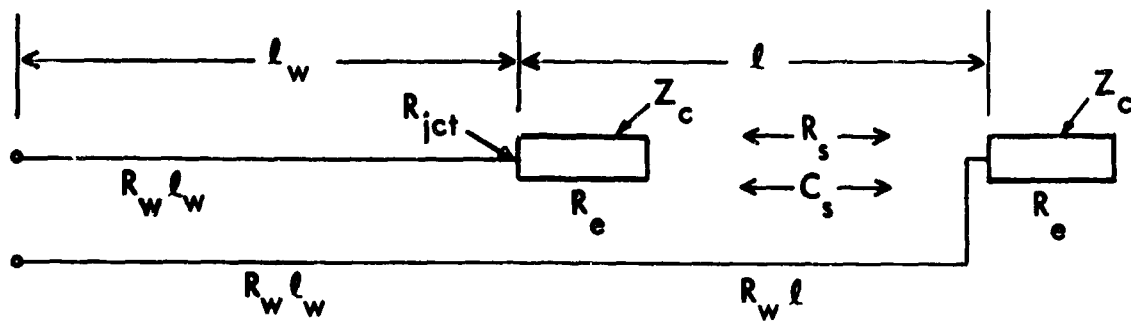


Figure C-1 Equivalent Circuit of a Dipole Antenna In Sea Water

would be the pair of electrodes immersed in the sea water or the electrode and the surrounding conducting shell in the proposed model system. The resulting induced voltage is given by the following formulas:

$$V_L = L_e E, \text{ volts}$$

where:

L_e = Voltage effective length of the sensing dipole, meters;

E = Total electric field, volts/meter.

It can be seen that the total electric field will consist of contributions from signals, atmospherics, earth currents, power system, hull currents and any other electric fields that may be propagating in the area. Thus, in Figure C-1, V_L represents the sum total voltage induced by all propagating fields.

APPENDIX D
VOLTAGE INDUCED INTO AN ELECTRIC
DIPOLE MOVING IN THE EARTH'S MAGNETIC FIELD

It will be shown below that an electric dipole which is moving through the sea will experience induced potentials by virtue of the dipole's movement in the earth's magnetic field. In the special case where the dipole is located at the surface of the sea, additional potentials will be developed the explanation of which is beyond the scope of this report. The present problem regards the totally submerged dipole in which the induced potentials, when divided by the dipole length, can be considered as an equivalent electric field strength which can then be compared with the field strengths of other ambient fields. It will be shown that under certain easily obtained conditions the equivalent electric field can be as high as several hundred microvolts per meter.

With particular attention being given to a pair of co-linear electrodes towed in the axial direction under the sea, it can be shown that voltages induced by pure linear translation (in the axial direction) are self cancelling; whereas, the voltages resulting from transverse rotation of the dipole axis do not cancel when the center of rotation is not at the center of the dipole. In fact, the largest induced voltages will be obtained when the dipole rotates about one end in such a way that the plane in which the dipole rotates is perpendicular to the magnetic field.

If the dipole is being towed at the end of a long cable, and the cable, due to unspecified perturbations, is snaking through the water, it can be seen that the direction of dipole axis will oscillate according to the oscillations of the tow line. In addition, other lateral forces such as unbalanced hydrodynamic forces at the electrodes can introduce oscillations of the dipole axis direction.

An analysis of the worst case begins by ignoring the self cancelling translational induction, and assuming that the dipole, a straight wire, is fixed at one end and rotates sinusoidally through an angle of $\pm \phi$ as shown in Figure D-1. The magnetic field is assumed to be uniform and nonvarying and oriented perpendicular to the plane of rotation (the x-y) plane. The angle of the wire

oscillates with a frequency Ω radians/second such that

$$\Theta = \phi \cos \Omega t. \quad (D-1)$$

where Θ is the angle of the dipole axis. Note that $|\Theta \text{ max}| = \phi$. The angular velocity of the wire is

$$\frac{d\Theta}{dt} = -\phi \Omega \sin \Omega t. \quad (D-2)$$

The tangential velocity of the elemental length dr at radius r is

$$\begin{aligned} V_r &= r \frac{d\Theta}{dt} \\ &= -r \phi \Omega \sin \Omega t. \end{aligned} \quad (D-3)$$

The voltage induced into the wire is then obtained from

$$\begin{aligned} v_i &= \oint \bar{V} \times \bar{B} \cdot d\bar{l} \\ &= \int_0^l (\bar{V} \times \bar{B}) \cdot d\bar{l} \\ &= \int_0^l V_r B \, dr. \end{aligned} \quad (D-4)$$

In equation (D-4) the path of integration is closed by taking the path a) from $l = 0$ to $l = l$ along the dipole, b) from $l = l$ back to $l = 0$ via a fixed external lead, or through the sea water. There are no voltages induced into the fixed return path, and so from equation (D-4), the total induced voltage is:

$$v_i = \frac{1}{2} B l^2 \phi \Omega \sin \Omega t. \quad (D-5)$$

In equation (D-5) the negative sign from equation (D-3) was dropped since it appears as an arbitrary polarity. Taking the value of magnetic flux density

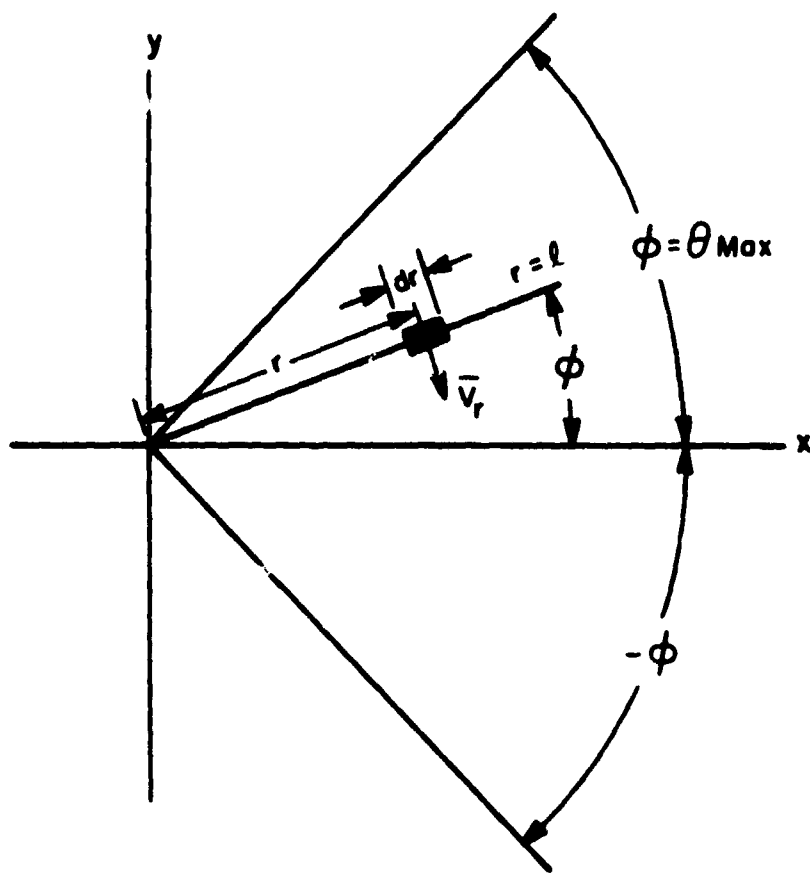


Figure D-1 Geometry for Wire Oscillating in a plane perpendicular to the Earth's Magnetic Field

as 5×10^{-5} webers/m², the root-mean-square level of the induced voltage is:

$$v_{i(\text{rms})} = 1.77 \times 10^{-5} l^2 \phi \Omega. \quad (\text{D-6})$$

The graph of equation (D-6) for some representative parameters is shown in Figure (D-2). From this it is seen that the motional noise at the antenna terminals can be significant if the oscillation frequency Ω falls sufficiently near the center frequency of the receiver. For example, if the angular frequency Ω is as high as 1.0 radian/sec, (6.28 cycles/sec.), and the total included angle is $\pi/8$ radians or 22.5° ($\phi = \pi/16$), then the rms voltage induced into a 100 meter dipole would be 3.5 millivolts at 6.28 cycles/second. This is equivalent to the voltage induced by an impressed electric field of 350 $\mu\text{v}/\text{meter}$. If the center frequency of the receiver is near 6 cycles/second, it is obvious that the motionally induced potentials would probably be several orders of magnitude greater than the observed ambient noise fields. Thus, the lower the carrier frequency and the wider the bandwidth, the more stringent are the requirements for the hydrodynamic stability of the tow line and electrodes.

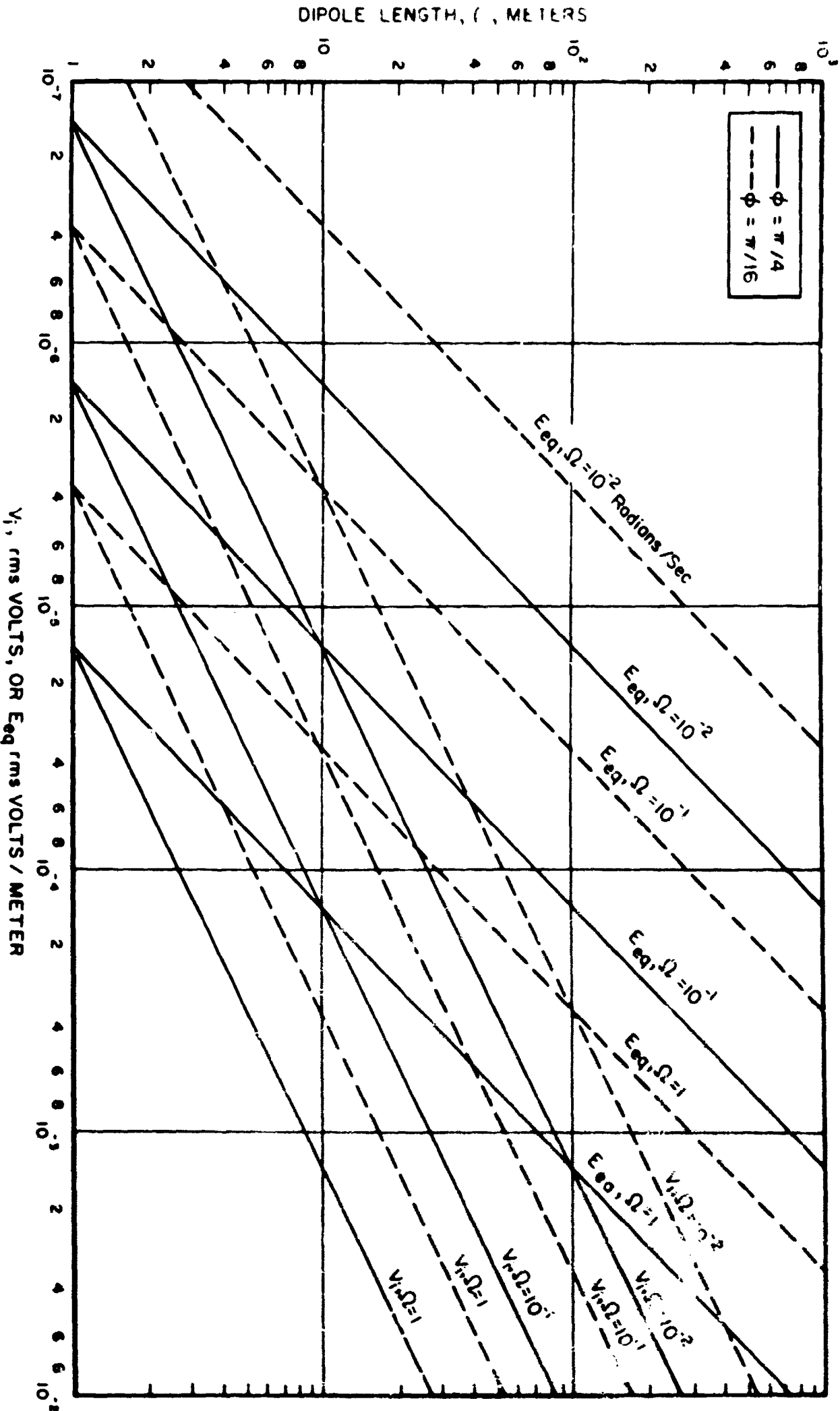


Figure D-2 Induced Voltage and Equivalent Electric Field Strength for an Electric Dipole Rotating in the Earth's Magnetic Field